

Review

Superconductors and Gravity

Antonio Gallerati ^{1,2,*}  and Giovanni Alberto Ummarino ^{1,3} 

¹ Dipartimento di Scienza Applicata e Tecnologia, Politecnico di Torino, Corso Duca degli Abruzzi 24, 10129 Torino, Italy; giovanni.ummarino@polito.it

² Istituto Nazionale di Fisica Nucleare, Sezione di Torino, Via Pietro Giuria 1, 10125 Torino, Italy

³ Institute for Physics and Engineering, National Research Nuclear University MPhI, Kashirskoe hwy 31, 115409 Moscow, Russia

* Correspondence: antonio.gallerati@polito.it

Abstract: We review and discuss some recent developments on the unconventional interaction between superconducting systems and the local gravitational field. While it is known that gravitational perturbations (such as gravitational waves) can affect supercondensates and supercurrents dynamics, we want to focus here on the more subtle superfluid back-reaction acting on the surrounding gravitational field, analysing some specific favourable situations. To this end, we will consider suitable quantum macrosystems in a coherent state, immersed in the static weak Earth's gravitational field, investigating possible slight local alterations of the latter not explained in terms of classical physics.

Keywords: Superconductivity; Gravitation; Macroscopic Quantum Effects; Graviton–Maxwell; Ginzburg–Landau



Citation: Gallerati, A.; Ummarino, G.A. Superconductors and Gravity. *Symmetry* **2022**, *14*, 554. <https://doi.org/10.3390/sym14030554>

Academic Editors: Ignatios Antoniadis and Kazuharu Bamba

Received: 20 January 2022

Accepted: 8 March 2022

Published: 10 March 2022

Publisher's Note: MDPI stays neutral with regard to jurisdictional claims in published maps and institutional affiliations.



Copyright: © 2022 by the authors. Licensee MDPI, Basel, Switzerland. This article is an open access article distributed under the terms and conditions of the Creative Commons Attribution (CC BY) license (<https://creativecommons.org/licenses/by/4.0/>).

1. Introduction

The gravitational force has the distinctive feature of universal interaction with all forms of matter and energy. It dominates at large-scales where it is well described by general relativity. In the latter theory, gravity is not interpreted as a standard force acting on different masses, but as a direct affection of the geometry of the spacetime: masses generate curvature, which in turn dictates the motion of the masses. The spacetime then plays a dynamical role and it is not a rigid background structure.

While classical general relativity gives a consistent description of the large-scale dynamics dominated by gravity, we know that quantum field theory is the fundamental formulation to describe physics at the microscopic scale, where the effects gravity are in general negligible. In the last few decades, different quantum gravity formulations have been proposed to consistently describe the physics of the particles when the gravitational field is so intense as to affect the motion of elementary particles (presumably in the vicinity of a black hole or a neutron star, as well as in the early stages of the evolution of our Universe). This is clearly an ambitious target, since it will imply a fundamental knowledge about the functioning of the laws of nature. However, experimental verification of this kind of theories is really hard to realize, since this would in general imply very high ranges of energy. Then, direct observation of quantum gravity effects, involving gravitons' dynamical interactions with other quantum fields at the microscopic level, is a very difficult task.

A different approach could originate from the study of unconventional, macroscopic states of matter. In this regard, one should consider quantum macrosystems existing in nature, like superconductors and superfluids. The latter can be thought as large systems featuring a macroscopical coherent phase, suitably described by order parameters. It could be then possible to formulate (and observe) a possible interplay between the extended,

coherent system and the surrounding gravitational field [1–21]. In this regard, the coupling with the current flow without resistance in superconductors was exploited to use the latter as a sensitive detection systems, in particular for gravitational waves [22–38]. Another remarkable phenomenon, showing quantum effects originating from the interaction of quantum particles with a weak-field gravitational background, is the gravity-induced quantum interference [39–48]. This effect takes place in the presence of a gravitational potential, to be considered in the Schrodinger equation [49,50] and giving rise to a phase shift for elementary particles (The experimental effect can be measured splitting a nearly monoenergetic beam of thermal particles and considering the produced interference paths: a gravity-induced quantum mechanical phase shift is observed, due to the presence of the Earth’s gravitational field [39,40]).

Inspired by the above results, we then also want to consider the back-reaction of superfluids and supercurrents on the local gravitational field in some specific, favourable situation. The first step to achieve the goal will be to formulate an appropriate theoretical model justifying this anomalous coupling. In the following subsections, we will briefly discuss the most convincing theoretical basis and experimental evidence in favour of the existence of this unconventional interaction.

1.1. Theoretical Foundations

We now want to characterize a possible interplay between superfluids and the local gravitational field in the framework of a quantum gravity theory or, at least, in a suitable approximation of the latter for weak fields.

Let us first consider the classical picture. Clearly, the absence of (gravitational) charges of opposite sign excludes the possibility of counteracting the field inside the medium by a local redistribution, ruling out dielectric-type effects. If we then take the medium to be a standard quantum mechanical system, the smallness of the gravitational coupling strongly suppresses the possibility of a (graviton) excitation for a medium particle and any subsequent affection of the local field. We are then led to consider the interaction of the gravitational field with an anomalous external source, that is, an unconventional state of matter exhibiting quantization on a macroscopic scale, like a Bose condensate or a more generic superfluid.

Let us then consider a quantum gravity framework and write the Lagrangian for this coherent macrosystem; immersed in the Earth’s gravitational field, (we work in the “mostly plus” convention, where the Minkowski metric is $\eta_{\mu\nu} = \text{diag}(-1, +1, +1, +1)$, and set $c = \hbar = 1$) [8,9]:

$$\mathcal{L} = \mathcal{L}_{\text{EH}} + \mathcal{L}_{\phi} = \frac{1}{8\pi G} (R - 2\Lambda) - \frac{1}{2} g^{\mu\nu} \partial_{\mu} \phi^* \partial_{\nu} \phi + \frac{1}{2} m^2 \phi^* \phi. \quad (1)$$

The first term is the Einstein–Hilbert contribution, R being the Ricci scalar and Λ the cosmological constant. The other terms describe the dynamics of the medium supercondensate (for example, Cooper pairs of mass m) that we can characterize as a bosonic field ϕ with non-vanishing vacuum expectation value (vev) $\phi_0 = \langle 0|\phi|0\rangle$. We assume this vev to be forced from the outside to a certain value, as it happens, for instance, in a superconductor subjected to external electromagnetic fields. In the weak gravity limit, the metric $g_{\mu\nu}$ can be written as

$$g_{\mu\nu}(x) = \eta_{\mu\nu} + h_{\mu\nu}(x), \quad (2)$$

sum of the flat Minkowski background $\eta_{\mu\nu}$ plus perturbations given by the $h_{\mu\nu}(x)$ contribution. Now, we expand the bosonic field as

$$\phi(x) = \phi_0(x) + \bar{\phi}(x), \quad (3)$$

where the ϕ_0 vev depends on the medium characteristics and can be seen as an external source, while the $\bar{\phi}$ contribution is included in the integration variables. The scalar field ϕ then suitably describes a superfluid with ground state density ϕ_0 fixed by external conditions (for example, Cooper pairs density in a supercondensate in the presence of external EM fields). In the weak gravity limit, the \mathcal{L}_ϕ term then reads

$$\mathcal{L}_\phi = \mathcal{L}_{\bar{\phi}} + \mathcal{L}_h + \mathcal{L}_0. \quad (4)$$

In the above expansion, the first term is related to the $\bar{\phi}$ contributions, involved in the negligible excitation processes related to the graviton emission–absorption mechanism, and several vertices of interaction that turn out to be irrelevant due to the smallness of the gravitational coupling. The second term takes into account the coupling of the condensate with the $h_{\mu\nu}$ metric fluctuations and is written as

$$\mathcal{L}_h \propto h^{\mu\nu} \partial_\mu \phi_0^* \partial_\nu \phi_0, \quad (5)$$

which determines corrections to the gravitational propagator, which is again a negligible contribution. Finally, the last term determines a local supercondensate contribution to the total effective cosmological term of the form

$$\mathcal{L}_0 = -\frac{1}{2} \partial_\mu \phi_0^* \partial^\mu \phi_0 + \frac{1}{2} m^2 |\phi_0|^2, \quad (6)$$

connected to the coherent vacuum energy density and depending on the fixed external source ϕ_0 . The above coupling has the correct structure to produce possible, localized instabilities in superfluid regions featuring larger condensate density [8,9]: this could determine detectable effects in spite of the smallness of the gravitational coupling. We should also note that, in the latter instable regions, some physical cutoff or regularizing process should come into play, preventing local contribution of arbitrary intensity (This can be considered a gravitational analog of the Casimir effect, where observable evidence originates from inhomogeneities in the vacuum fluctuations. In the latter case, the metallic conductors impose a cutoff on the electromagnetic vacuum fluctuations, while the same role is played here by the coherent superfluid). The field then tends to be pinned, assuming fixed extremal values which are independent from those in the neighbouring regions. One could expect, as a physical effect, some kind of slight partial shielding (“absorption”) locally affecting fields propagation and potentials. As we already pointed out, the introduced superfluid density $\phi_0(x)$ is related to the microscopic structure of the involved sample, as well as to the presence of currents, vortex lattices and electromagnetic fields in the supercondensate (It has also been conjectured that high-frequency electromagnetic fields could provide the required energy to enhance the described gravitational field affection [8,15]).

We have then described a theoretical quantum gravity model with an unconventional coupling between the local gravitational field and the superfluid. The existence of strong variations of the supercondensate components density (for example, Cooper pairs) produce small regions with higher density, where a criticality condition could take place, giving rise to localized instabilities. This gives us a possible way to elude the weakness of the standard coupling and produce a related affection of the local gravitational field. The key ingredient is the macroscopic quantum coherence of the condensate that is taken into account when computing the anomalous interplay, at a fundamental level, between the superfluid and the external gravitational field.

1.2. Experimental Evidence

The discussed formulation laid the foundations of a theoretical approach to an unconventional coupling between superfluids and gravity, in the framework of a quantum model. This, however, involves a formalism that makes it almost impossible to extract quantitative predictions, to be tested in a laboratory experiment. For this reason, one is then led to also consider many phenomenological research reports and evidence, to better understand the proposed interplay and obtain an effective theory leading to more explicit experimental predictions.

One of the first attempts to formulate an effective quantum model describing the interaction between conductors and the local gravitational field was given in [51], where a quantum-mechanical formalism is developed to calculate an (additional) electric field component, generated in the vicinity of a conductor by the presence of the Earth's gravity. The main consequence of this formulation is the definition of generalized electric-type fields and potentials, existing near the surface of a conductor and featuring a gravitationally-induced component. We can schematically express this generalized field as

$$\mathbf{E} = \mathbf{E}_e + \mathbf{E}_{\text{ind}} \quad V = V_e + V_{\text{ind}} \quad (7)$$

where \mathbf{E}_e is the standard electric field, while \mathbf{E}_{ind} is the gravitationally-induced component. In [52,53], the induced \mathbf{E}_{ind} and V_{ind} were experimentally detected as a direct affection to the free fall of electrons in the presence of conductors. This evidence of existence of generalized fields and potentials was then theoretically analysed and experimentally verified in subsequent works [54–61].

Analogous concepts were subsequently extended to superconductors, obtaining similar results [11,33,62–73]: generalized gravitoelectric and gravitomagnetic fields can be induced by the presence of a local gravitational field coupled to the supercondensate.

In the following section, we discuss a formal derivation of a consistent form for these generalized fields and potentials, exploiting a weak field expansion for the local gravitational field. This approach will lead us to the definition of a generalized form for Maxwell equations.

2. Linearized Gravity: Gravito–Maxwell Fields

It is well known that gravity is in general mediated by a symmetric $g_{\mu\nu}$ tensor field, featuring 10 independent components (potentials). However, under certain approximations and suitable gauge choice, the gravitational field behaviour can be described in an electromagnetic-like fashion, by means of vector-like field equations instead of the corresponding tensorial expressions. In particular, linearized gravity can be considered as a consistent weak-field limit of the complete tensorial theory, in the regime where nonlinear effects can be ignored (In the linear-order assumption, the gravitational field does not transfer energy to the gravitational sources; this also cancels matter–gravity coupling from the domain of linear approximations).

Let us consider a nearly-flat spacetime, characterized by the presence of a weak and static gravitational field. This means we can consider small perturbation of the Minkowski metric $\eta_{\mu\nu}$ and express the spacetime metric $g_{\mu\nu}$ as

$$g_{\mu\nu} \simeq \eta_{\mu\nu} + h_{\mu\nu} , \quad (8)$$

where the symmetric tensor $h_{\mu\nu}$ is a small perturbation of the constant flat $\eta_{\mu\nu}$ in the mostly plus convention, $\eta_{\mu\nu} = \text{diag}(-1, +1, +1, +1)$. The inverse metric, in linear approximation, is given by

$$g^{\mu\nu} \simeq \eta^{\mu\nu} - h^{\mu\nu} . \quad (9)$$

while the metric determinant can be expanded as

$$g = \det[g_{\mu\nu}] = \varepsilon^{\mu\nu\rho\sigma} g_{1\mu} g_{2\nu} g_{3\rho} g_{4\sigma} \simeq -1 - h \Rightarrow \sqrt{-g} \simeq 1 + \frac{1}{2} h, \tag{10}$$

where $h = h^\sigma_\sigma$.

We are now going to exploit the above weak-limit expansion of the metric to obtain a linearized form for the Einstein and London equations. We will then take advantage of the obtained results to define suitable backgrounds to test the discussed gravity/superfluid interplay.

2.1. Generalizing Maxwell Equations

Let us put ourselves in an inertial coordinate system. To first order in $h_{\mu\nu}$, the connection is expanded as

$$\Gamma^\lambda_{\mu\nu} \simeq \frac{1}{2} \eta^{\lambda\rho} (\partial_\mu h_{\nu\rho} + \partial_\nu h_{\rho\mu} - \partial_\rho h_{\mu\nu}). \tag{11}$$

The Riemann tensor is defined as:

$$R^\sigma_{\mu\lambda\nu} = \partial_\lambda \Gamma^\sigma_{\mu\nu} - \partial_\nu \Gamma^\sigma_{\mu\lambda} + \Gamma^\sigma_{\rho\lambda} \Gamma^\rho_{\nu\mu} - \Gamma^\sigma_{\rho\nu} \Gamma^\rho_{\lambda\mu}, \tag{12}$$

while the Ricci tensor is obtained from the contraction

$$R_{\mu\nu} = R^\sigma_{\mu\sigma\nu}, \tag{13}$$

and, to linear order in $h_{\mu\nu}$, it is expressed as

$$\begin{aligned} R_{\mu\nu} &\simeq \partial_\sigma \Gamma^\sigma_{\mu\nu} + \partial_\mu \Gamma^\sigma_{\sigma\nu} + \mathcal{F}\mathcal{F} - \mathcal{F}\mathcal{F} \\ &= \frac{1}{2} (\partial_\mu \partial^\rho h_{\nu\rho} + \partial_\nu \partial^\rho h_{\mu\rho}) - \frac{1}{2} \partial_\rho \partial^\rho h_{\mu\nu} - \frac{1}{2} \partial_\mu \partial_\nu h \\ &= \partial^\rho \partial_{(\mu} h_{\nu)\rho} - \frac{1}{2} \partial^2 h_{\mu\nu} - \frac{1}{2} \partial_\mu \partial_\nu h, \end{aligned} \tag{14}$$

having used Equation (11).

The Einstein equations are written as:

$$R_{\mu\nu} - \frac{1}{2} g_{\mu\nu} R = 8\pi G T_{\mu\nu}, \tag{15}$$

where $R = g^{\mu\nu} R_{\mu\nu}$ is the Ricci scalar. In linear-order approximation, we have

$$\frac{1}{2} g_{\mu\nu} R \simeq \frac{1}{2} \eta_{\mu\nu} \eta^{\rho\sigma} R_{\rho\sigma} = \frac{1}{2} \eta_{\mu\nu} (\partial^\rho \partial^\sigma h_{\rho\sigma} - \partial^2 h), \tag{16}$$

having used Equation (14). The l.h.s. of (15) then reads

$$R_{\mu\nu} - \frac{1}{2} g_{\mu\nu} R \simeq \partial^\rho \partial_{(\mu} h_{\nu)\rho} - \frac{1}{2} \partial^2 h_{\mu\nu} - \frac{1}{2} \partial_\mu \partial_\nu h - \frac{1}{2} \eta_{\mu\nu} (\partial^\rho \partial^\sigma h_{\rho\sigma} - \partial^2 h). \tag{17}$$

Let us now introduce the symmetric traceless tensor

$$\bar{h}_{\mu\nu} = h_{\mu\nu} - \frac{1}{2} \eta_{\mu\nu} h, \tag{18}$$

so that (17) is rewritten as

$$\begin{aligned}
 R_{\mu\nu} - \frac{1}{2} g_{\mu\nu} R &\simeq \frac{1}{2} (\partial^\rho \partial_\mu \bar{h}_{\nu\rho} + \partial^\rho \partial_\nu \bar{h}_{\mu\rho} - \partial^\rho \partial_\rho \bar{h}_{\mu\nu} - \eta_{\mu\nu} \partial^\rho \partial^\sigma \bar{h}_{\rho\sigma}) \\
 &= \partial^\rho \partial_{[\nu} \bar{h}_{\rho]\mu} + \partial^\rho \partial^\sigma \eta_{\mu[\sigma} \bar{h}_{\nu]\rho} \\
 &= \partial^\rho (\partial_{[\nu} \bar{h}_{\rho]\mu} + \partial^\sigma \eta_{\mu[\rho} \bar{h}_{\nu]\sigma}).
 \end{aligned}
 \tag{19}$$

We also define the tensor

$$\mathcal{G}_{\mu\nu\rho} \equiv \partial_{[\nu} \bar{h}_{\rho]\mu} + \partial^\sigma \eta_{\mu[\rho} \bar{h}_{\nu]\sigma},
 \tag{20}$$

in terms of which the Einstein equations take the compact form:

$$\partial^\rho \mathcal{G}_{\mu\nu\rho} = 8\pi G T_{\mu\nu}.
 \tag{21}$$

2.1.1. Gauge Fixing

We now consider the *harmonic coordinate condition*, expressed by the relation [74,75]:

$$\partial_\mu (\sqrt{-g} g^{\mu\nu}) = 0 \quad \Leftrightarrow \quad \square x^\mu = 0,
 \tag{22}$$

that in turn can be rewritten in the form

$$g^{\mu\nu} \Gamma^\lambda_{\mu\nu} = 0,
 \tag{23}$$

also known as *De Donder gauge*. The requirement of the above coordinate condition (22) then plays the role of gauge fixing. In particular, in harmonic coordinates, the metric satisfies a manifestly Lorenz-covariant condition, so that the De Donder gauge becomes a natural choice. Moreover, if one considers the weak-field expansion of the Einstein–Hilbert action in De Donder gauge, the action itself (as well as the graviton propagator) takes a particularly simple form.

Using Equations (8) and (11) together with the above gauge fixing (23), in first-order approximation, we find:

$$0 \simeq \frac{1}{2} \eta^{\mu\nu} \eta^{\lambda\rho} (\partial_\mu h_{\nu\rho} + \partial_\nu h_{\rho\mu} - \partial_\rho h_{\mu\nu}) = \partial_\mu h^{\mu\lambda} - \frac{1}{2} \partial^\lambda h,
 \tag{24}$$

that in turn implies the condition

$$\partial_\mu h^{\mu\nu} \simeq \frac{1}{2} \partial^\nu h \quad \Leftrightarrow \quad \partial^\mu h_{\mu\nu} \simeq \frac{1}{2} \partial_\nu h.
 \tag{25}$$

We can also write

$$\partial^\mu h_{\mu\nu} = \partial^\mu \left(\bar{h}_{\mu\nu} + \frac{1}{2} \eta_{\mu\nu} h \right) = \partial^\mu \bar{h}_{\mu\nu} + \frac{1}{2} \partial_\nu h,
 \tag{26}$$

so that, using Equation (25), we obtain the *Lorentz gauge condition*:

$$\partial^\mu \bar{h}_{\mu\nu} \simeq 0.
 \tag{27}$$

This condition further simplifies Equation (20) for $\mathcal{G}_{\mu\nu\rho}$, which takes the simple form

$$\mathcal{G}_{\mu\nu\rho} \simeq \partial_{[\nu} \bar{h}_{\rho]\mu},
 \tag{28}$$

and satisfies the relation

$$\partial_{[\lambda|\mathcal{G}_{0|\mu\nu]} = 0 \Rightarrow \mathcal{G}_{0\mu\nu} \propto \partial_\mu A_\nu - \partial_\nu A_\mu, \tag{29}$$

The above expression then suggests the existence of a potential. In the following paragraphs, we are going to analyse in detail suitable expressions for fields and potentials defining the desired formalism.

2.1.2. Gravito–Maxwell Equations

Let us now define the following fields [19,63,68,76,77] (for the sake of simplicity, we initially set the physical charge $e = m = 1$)

$$\mathbf{E}_g \equiv E_i = -\frac{1}{2} \mathcal{G}_{00i} = -\frac{1}{2} \partial_{[0} \bar{h}_{i]0}, \tag{30a}$$

$$\mathbf{A}_g \equiv A_i = \frac{1}{4} \bar{h}_{0i}, \tag{30b}$$

$$\mathbf{B}_g \equiv B_i = \frac{1}{4} \varepsilon_i{}^{jk} \mathcal{G}_{0jk}, \tag{30c}$$

with $i = 1, 2, 3$ and

$$\mathcal{G}_{0ij} = \partial_{[i} \bar{h}_{j]0} = \frac{1}{2} (\partial_i \bar{h}_{j0} - \partial_j \bar{h}_{i0}) = 4 \partial_{[i} A_{j]}. \tag{31}$$

From the above definitions, it follows that

$$\mathbf{B}_g = \frac{1}{4} \varepsilon_i{}^{jk} 4 \partial_{[j} A_{k]} = \varepsilon_i{}^{jk} \partial_j A_k = \nabla \times \mathbf{A}_g, \tag{32}$$

that also implies

$$\nabla \cdot \mathbf{B}_g = 0. \tag{33}$$

We then also find

$$\nabla \cdot \mathbf{E}_g = \partial^i E_i = -\partial^i \frac{\mathcal{G}_{00i}}{2} = -8\pi G \frac{T_{00}}{2} = 4\pi G \rho_g, \tag{34}$$

having used Equation (21) and defined the mass density as $\rho_g \equiv -T_{00}$.

We then consider the curl of \mathbf{E}_g :

$$\begin{aligned} \nabla \times \mathbf{E}_g &= \varepsilon_i{}^{jk} \partial_j E_k = -\varepsilon_i{}^{jk} \partial_j \frac{\mathcal{G}_{00k}}{2} = -\frac{1}{2} \varepsilon_i{}^{jk} \partial_j \partial_{[0} \bar{h}_{k]0} \\ &= -\frac{1}{4} 4 \partial_0 \varepsilon_i{}^{jk} \partial_j A_k = -\partial_0 B_i = -\frac{\partial \mathbf{B}_g}{\partial t}. \end{aligned} \tag{35}$$

Finally, for the curl of \mathbf{B}_g , we find

$$\begin{aligned} \nabla \times \mathbf{B}_g &= \varepsilon_i{}^{jk} \partial_j B_k = \frac{1}{4} \varepsilon_i{}^{jk} \varepsilon_k{}^{\ell m} \partial_j \mathcal{G}_{0\ell m} = \frac{1}{4} (\delta_i{}^\ell \delta^{jm} - \delta_i{}^m \delta^{j\ell}) \partial_j \mathcal{G}_{0\ell m} \\ &= \frac{1}{2} \partial^j \mathcal{G}_{0ij} = \frac{1}{2} (\partial^\mu \mathcal{G}_{0i\mu} + \partial_0 \mathcal{G}_{0i0}) = \frac{1}{2} (\partial^\mu \mathcal{G}_{0i\mu} - \partial_0 \mathcal{G}_{00i}) \\ &= \frac{1}{2} (8\pi G T_{0i} - \partial_0 \mathcal{G}_{00i}) = 4\pi G j_i + \frac{\partial E_i}{\partial t} = 4\pi G \mathbf{j}_g + \frac{\partial \mathbf{E}_g}{\partial t}, \end{aligned} \tag{36}$$

having used again Equation (21) and defined the mass gravito-current density vector as

$$\mathbf{j}_g \equiv j_i \equiv T_{0i}.$$

In summary, the fields (30) are defined, one can write the field equations [11,19,28,32,63,67,68,76,78–91]:

$$\begin{aligned}\nabla \cdot \mathbf{E}_g &= 4\pi G \rho_g, \\ \nabla \cdot \mathbf{B}_g &= 0, \\ \nabla \times \mathbf{E}_g &= -\frac{\partial \mathbf{B}_g}{\partial t}, \\ \nabla \times \mathbf{B}_g &= \frac{4\pi G}{c^2} \mathbf{j}_g + \frac{1}{c^2} \frac{\partial \mathbf{E}_g}{\partial t},\end{aligned}\quad (37)$$

having restored physical units. The above expressions are formally equivalent to Maxwell equations, with \mathbf{E}_g and \mathbf{B}_g being the gravitoelectric and gravitomagnetic field, respectively (For instance, on the Earth's surface, \mathbf{E}_g corresponds to the Newtonian gravitational acceleration, while \mathbf{B}_g is related to angular momentum interactions [63,68,78,81]). The mass current density vector \mathbf{j}_g can also be written as:

$$\mathbf{j}_g = \rho_g \mathbf{v}, \quad (38)$$

in terms of the mass density and velocity \mathbf{v} .

2.1.3. Generalized Maxwell Equations

Inspired by the discussion of Section 1.2, it is now straightforward to extend the above results and introduce generalized electric/magnetic fields, scalar and vector potentials. The latter feature both electromagnetic and gravitational contributions and can be written as:

$$\mathbf{E} = \mathbf{E}_e + \frac{m}{e} \mathbf{E}_g \quad \mathbf{B} = \mathbf{B}_e + \frac{m}{e} \mathbf{B}_g \quad V = V_e + \frac{m}{e} V_g \quad \mathbf{A} = \mathbf{A}_e + \frac{m}{e} \mathbf{A}_g \quad (39)$$

where m and e are the electron mass and charge, respectively [51].

The generalized Maxwell equations then become:

$$\begin{aligned}\nabla \cdot \mathbf{E} &= \left(\frac{1}{\varepsilon_g} + \frac{1}{\varepsilon_0} \right) \rho, \\ \nabla \cdot \mathbf{B} &= 0, \\ \nabla \times \mathbf{E} &= -\frac{\partial \mathbf{B}}{\partial t}, \\ \nabla \times \mathbf{B} &= (\mu_g + \mu_0) \mathbf{j} + \frac{1}{c^2} \frac{\partial \mathbf{E}}{\partial t},\end{aligned}\quad (40)$$

where ε_0 and μ_0 are the standard electric permittivity and magnetic permeability in the vacuum, and where we have set

$$\rho_g = \frac{m}{e} \rho, \quad \mathbf{j}_g = \frac{m}{e} \mathbf{j}, \quad (41)$$

ρ and \mathbf{j} being the electric charge density and electric current density, respectively. The introduced vacuum gravitational permittivity ε_g and vacuum gravitational permeability μ_g are defined as

$$\varepsilon_g = \frac{1}{4\pi G} \frac{e^2}{m^2}, \quad \mu_g = \frac{4\pi G}{c^2} \frac{m^2}{e^2}. \quad (42)$$

The obtained generalized Maxwell equations turn out to be a consistent approximation to the complete tensorial theory, valid in the limit of the weak gravitational field (like the static, weak Earth's gravity). It is then possible to take advantage of the obtained results and consider suitable situations and parameters regime where the gravitoelectric field plays a fundamental role and/or where gravitomagnetic effects are not negligible.

2.2. Generalizing London Equations

The London equations for a superconductor in stationary state characterize an analogous Ohm's law (zero resistivity) and Meissner effect (expulsion of the magnetic field from the interior sample) for the superfluid. They can be explicitly written as [92–94]:

$$\mathbf{E}_e = -\frac{m}{n_s e^2} \frac{\partial \mathbf{j}}{\partial t}; \quad (43)$$

$$\mathbf{B}_e = -\frac{m}{n_s e^2} \nabla \times \mathbf{j}. \quad (44)$$

where $\mathbf{j} = n_s e v_s$ is the supercurrent and n_s is the superelectron density.

The Ampère's law for a superconductor in stationary state (no displacement current) has the form

$$\nabla \times \mathbf{B}_e = \mu_0 \mathbf{j}, \quad (45)$$

so that taking the curl gives

$$\nabla \times \nabla \times \mathbf{B}_e = \nabla(\nabla \cdot \mathbf{B}_e) - \nabla^2 \mathbf{B}_e = \mu_0 \nabla \times \mathbf{j} = -\frac{\mu_0 n_s e^2}{m} \mathbf{B}_e, \quad (46)$$

that is,

$$\nabla^2 \mathbf{B}_e = \frac{1}{\lambda_e^2} \mathbf{B}_e, \quad (47)$$

having introduced the penetration depth

$$\lambda_e = \sqrt{\frac{m}{\mu_0 n_s e^2}}. \quad (48)$$

The above quantity gives an estimate of the mean distance the magnetic field \mathbf{B}_e can penetrate the sample. Since the values of the λ_e parameter vary from 2 nm (low T_c superconductors) to 200 nm (high T_c superconductors), the above Equations (47) and (48) quantitatively characterize the Meissner effect.

The two London Equations (43) and (44) can be now rewritten in terms of the vector potential \mathbf{A}_e in the (not gauge-invariant) form:

$$\mathbf{j} = -\frac{1}{\mu_0 \lambda_e^2} \mathbf{A}_e \quad (49)$$

with $\mathbf{B}_e = \nabla \times \mathbf{A}_e$ and expressing the electric field as $\mathbf{E}_e = -\frac{\partial \mathbf{A}_e}{\partial t}$.

Generalized London Equations

Let us now take into account gravitational contributions, and consider for the fields and potentials the generalized form (39). In particular, we consider the generalized potential \mathbf{A} minimally coupled to the wave function

$$\psi = \psi_0 \exp(i\varphi) \quad \psi_0^2 \equiv |\psi|^2 = n_s. \quad (50)$$

The second London equation can be derived from the quantum mechanical current density

$$\mathbf{j} = -\frac{i}{2m}(\psi^* \tilde{\nabla} \psi - \psi \tilde{\nabla} \psi^*), \tag{51}$$

where $\tilde{\nabla}$ is the covariant derivative for the minimal coupling:

$$\tilde{\nabla} = \nabla - i \tilde{g} \mathbf{A}, \tag{52}$$

with unknown coupling constant \tilde{g} . We then find for the current

$$\mathbf{j} = -\frac{i}{2m}(\psi^* \nabla \psi - \psi \nabla \psi^*) - \frac{\tilde{g}}{m} \mathbf{A} |\psi|^2 = \frac{1}{m} |\psi|^2 (\nabla \varphi - \tilde{g} \mathbf{A}). \tag{53}$$

Now, taking the curl of the previous expression gives

$$\mathbf{B} = -\frac{m}{\tilde{g} |\psi|^2} \nabla \times \mathbf{j} = -\frac{1}{\zeta} \nabla \times \mathbf{j}, \tag{54}$$

which is the generalized form of the second London Equation (44) [79].

We now want to fix the values of the ζ parameter and coupling constant \tilde{g} . To this end, let us restrict to the case $\mathbf{B}_g = 0$:

$$\mathbf{B} = \mathbf{B}_e + \frac{m}{e} \cancel{\mathbf{B}_g} = -\frac{1}{\zeta} \nabla \times \mathbf{j}, \tag{55}$$

so that, using (44), (48) and (50), we find

$$\tilde{g} = e^2 \quad \frac{1}{\zeta} = \mu_0 \lambda_e^2. \tag{56}$$

In order to define an analogue gravitational penetration depth, we now consider the case $\mathbf{B}_e = 0$:

$$\mathbf{B} = \cancel{\mathbf{B}_e} + \frac{m}{e} \mathbf{B}_g = -\mu_0 \lambda_e^2 \nabla \times \mathbf{j} = -\mu_0 \lambda_e^2 \frac{m}{e} \nabla \times \mathbf{j}_g, \tag{57}$$

the gravito-Ampère’s law (37) in stationary state reading

$$\nabla \times \mathbf{B}_g = \mu_g \mathbf{j}_g. \tag{58}$$

Taking the curl of the above equation, we have

$$\nabla \times \nabla \times \mathbf{B}_g = -\nabla^2 \mathbf{B}_g = \mu_g \nabla \times \mathbf{j}_g = -\mu_g \frac{1}{\mu_0 \lambda_e^2} \mathbf{B}_g = -\frac{1}{\lambda_g^2} \mathbf{B}_g, \tag{59}$$

having introduced the gravitational penetration depth

$$\lambda_g = \sqrt{\frac{\mu_0 \lambda_e^2}{\mu_g}} = \sqrt{\frac{c^2}{4\pi G m n_s}}. \tag{60}$$

Writing now the stationary generalized Ampère’s law (40) and using Equation (60), we obtain

$$\nabla \times \mathbf{B} = (\mu_0 + \mu_g) \mathbf{j} = \mu_0 \left(1 + \frac{\lambda_e^2}{\lambda_g^2} \right) \mathbf{j}, \tag{61}$$

and, taking the curl, we find the general form

$$\begin{aligned} \nabla^2 \mathbf{B} &= -\mu_0 \left(1 + \frac{\lambda_e^2}{\lambda_g^2} \right) \nabla \times \mathbf{j} = \mu_0 \frac{1}{\mu_0 \lambda_e^2} \left(1 + \frac{\lambda_e^2}{\lambda_g^2} \right) \mathbf{B} = \\ &= \left(\frac{1}{\lambda_e^2} + \frac{1}{\lambda_g^2} \right) \mathbf{B} = \frac{1}{\lambda^2} \mathbf{B}, \end{aligned} \tag{62}$$

where we have introduced the *generalized penetration depth* λ :

$$\lambda = \frac{\lambda_g \lambda_e}{\sqrt{\lambda_g^2 + \lambda_e^2}} \simeq \lambda_e, \quad \text{with } \frac{\lambda_g}{\lambda_e} \simeq 10^{21}. \tag{63}$$

Finally, we can recast Equation (49) in the form

$$\mathbf{j} = -\zeta \mathbf{A}, \tag{64}$$

with $\mathbf{B} = \nabla \times \mathbf{A}$. Moreover, since charge-conservation requires the condition $\nabla \cdot \mathbf{j} = 0$, we obtain for the vector potential

$$\nabla \cdot \mathbf{A} = 0,$$

that is, the so-called *Coulomb gauge* (or *London gauge*).

In the following sections, we are going to consider suitable frameworks where the proposed gravity/superfluid interplay can in principle be detected, precisely characterizing the physical system and optimizing the range of parameters in order to maximize the effect. We will also exploit the described formalism and introduce generalized fields.

3. A Simple Application: Josephson Effect

The Josephson effect consists of the transmission of supercurrents through thin insulating barriers by means of quantum-mechanical tunnelling [95]. The phenomenon can be seen as a general property of coupled superconducting systems and could take place in suitable tunnel junctions, where quantum interference appears. In particular, when the states of two superconductors are assumed to be coherent (that is, coherent superpositions of states with different numbers of particle pairs), there exists a phase-dependent coupling energy between the two. The latter then implies the possibility of a supercurrent flowing across the junction [96].

3.1. Josephson Junction

If two superconductors are put in contact and the critical current in the contact region is well below those of the individual constituents, the configuration is defined as *weak link*. Once the weak link is formed, coherence is established across the barrier, with a phase difference $\Delta\varphi$ causing interference between the previously independent wavefunctions, so that the system can be described with a single wavefunction as a whole.

When two superconducting samples are connected through a weak Josephson link, the response of the supercondensate (through the corresponding coupling energy) keeps the macroscopic internal coherence of the system, allowing direct observation of coherence–interference phenomena. In particular, a simple manifestation of the Josephson effect can be observed in a circuit closed on a superconductor–insulator–superconductor (SIS) junction, to which a constant potential difference ΔV is applied. The voltage, in turn, produces a sinusoidal superconductive current across the junction with pulsation [95–97]

$$\omega = \frac{2e\Delta V}{\hbar}. \quad (65)$$

Let us briefly discuss the phenomenon.

Josephson AC Current

Let us consider a weak link between two superconductors. The latter, when taken separately, are described by wavefunctions of phases φ_1 , φ_2 and amplitudes $|\psi_1|$, $|\psi_2|$. We can explicitly write

$$\begin{aligned} \psi_1 &= |\psi_1| \exp(i\varphi_1) = \sqrt{\rho_1} \exp(i\varphi_1), \\ \psi_2 &= |\psi_2| \exp(i\varphi_2) = \sqrt{\rho_2} \exp(i\varphi_2), \end{aligned} \quad (66)$$

where ρ_1, ρ_2 are the probability amplitudes of Cooper pair densities.

Once the weak link is formed, coherence is established across the barrier, and the phase difference

$$\Delta\varphi = \varphi_2 - \varphi_1 = \gamma \quad (67)$$

determines interference between the (previously independent wavefunctions), so that the system can be described by means of a single wavefunction as a whole.

An SIS tunnel Josephson junction is a typical weak link consisting of two superconductors (that we take equal for simplicity) of thickness L and surface A , separated by a thin oxide layer of thickness $\ell \ll L$, see Figure 1. The time dependent Schrodinger equation can be used to characterize the system evolution as

$$i\hbar \frac{\partial\psi}{\partial t} = \mathcal{E} \psi. \quad (68)$$

As we already discussed, in the weak link, a coherent overlap takes place between the two wavefunctions, and an additional term must be added to take into account the interaction. In particular, the rate of change of ψ_1 is proportional to its coupling to ψ_2 , the same happening for ψ_2 on the other side. It is then possible to write the relations [98]

$$i\hbar \frac{\partial\psi_1}{\partial t} = \mathcal{E}_1 \psi_1 + K \psi_2, \quad (69)$$

$$i\hbar \frac{\partial\psi_2}{\partial t} = \mathcal{E}_2 \psi_2 + K \psi_1. \quad (70)$$

For the sake of simplicity, we will consider a superconductor of the same kind, so that the probability amplitudes of Cooper pair densities are equal, $\rho_1 = \rho_2 = \rho$. The quantities \mathcal{E}_1 and \mathcal{E}_2 are the ground state energies of the unperturbed system (i.e. when $K = 0$) and we choose the zero of energy to be halfway between \mathcal{E}_1 and \mathcal{E}_2 , the evolution of the system then depending on the difference $\Delta\mathcal{E} = \mathcal{E}_2 - \mathcal{E}_1$.

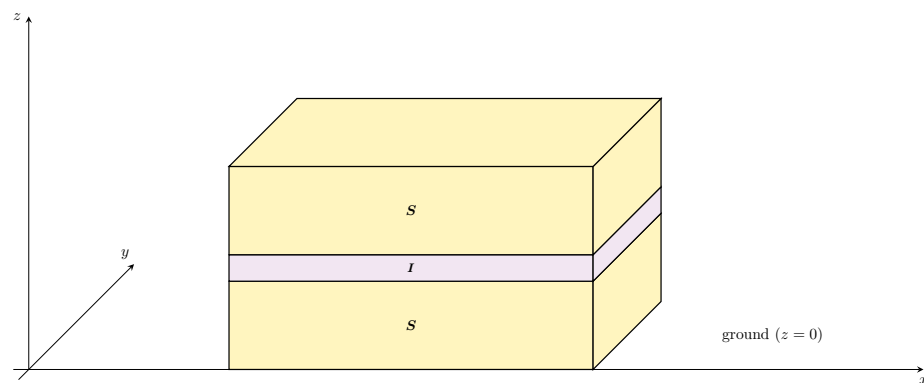


Figure 1. SIS junction with an axis directed along the z -direction, parallel to the local Earth’s gravitational field.

Now, we put expressions (66) in the evolution relations Equations (69) and (70), assuming each wavefunction having a well-defined Cooper pair density and space-independent macroscopic phase. Separating the real and imaginary part, we find:

$$\frac{\partial \gamma}{\partial t} = \frac{\Delta \mathcal{E}}{\hbar} = 0, \quad (71)$$

$$\frac{\partial \rho}{\partial t} = \frac{2K}{\hbar} \rho \sin(\gamma), \quad (72)$$

with $\gamma = \varphi_2 - \varphi_1$, the expression being valid in the absence of applied voltage of any kind (electric or gravitational-like) (Equation (72) is written in the standard Josephson formalism [99] with a little abuse of notation: the ρ -density involved in the time-derivative on the l.h.s. refers to the superconducting current density across the interface, while the density on the r.h.s. refers to the global density of Cooper pairs in the system; the latter is a conserved (constant) quantity, being the system in the superconductive state). The supercurrent across the contact then is written

$$J_s = -2e \frac{\partial \rho}{\partial t} = -\frac{4eK}{\hbar} \rho \sin(\gamma) = J_0 \sin(\gamma), \quad (73)$$

flowing through the thin layer separating the superconductors and depending on the phase difference across the barrier.

If we apply a constant voltage ΔV across the junction, an oscillatory variation of phase difference takes place. A corresponding AC supercurrent then appears in the weak link, due to the existing finite potential difference in the junction. The phenomenon is a manifestation of the Josephson–Gor’kov principle [96,100,101], which simply states that the oscillation frequency of the coherent matter field is driven by the existing chemical potential (corresponding to pairs of electrons in the case of superconductivity). Since the supercurrent is a periodic function of $\Delta \varphi$, AC supercurrents must be associated with any applied voltage difference (general principle of gauge invariance dictates that all physical properties must be periodic functions of the phase with period 2π). Equation (71) is then modified in order to take into account the applied voltage, resulting in a time-dependent relation of the form [95–97,101,102]:

$$\frac{\partial \gamma}{\partial t} = \frac{2e\Delta V}{\hbar}, \quad (74)$$

relating the phase difference variation on opposite sides to the existing potential difference across the junction. After integration, the above (74) gives

$$\gamma(t) = \gamma_0 + \frac{2e\Delta V}{\hbar}t, \tag{75}$$

γ_0 being an integration constant. The supercurrent density turns out to be

$$J_s = I_0 \sin\left(\gamma_0 + \frac{2e\Delta V}{\hbar}t\right). \tag{76}$$

and, below the critical temperature, the amplitude of the corresponding tunnelling supercurrent $I_0 = J_0 A$ is temperature-dependent and is expressed by the Ambegaokar–Baratoff formula [103,104]:

$$I_0 = \frac{\pi \Delta_S(T)}{2eR_N} \tanh\left(\frac{\Delta_S(T)}{2k_B T}\right), \tag{77}$$

where R_N is the junction resistance in the normal state and $\Delta_S(T)$ is the superconductive gap. The described AC signal, coming from the applied DC voltage, may be understood as the result of the energy conversion of electron pairs into photons [105].

In the following, we will examine the possibility of a Josephson-like effect induced by the weak-static Earth’s gravitational field, also analysing suitable experimental settings and parameter optimization.

3.2. Josephson Effect Induced by Gravity

We have discussed and motivated in the previous sections the introduction of generalized electric field and potential of the form

$$\mathbf{E} = \mathbf{E}_e + \frac{m}{e} \mathbf{E}_g \quad V = V_e + \frac{m}{e} V_g. \tag{78}$$

If we now restrict to a simple situation in which it is present only the Earth’s static gravitational field ($\mathbf{E}_e = 0$), we have that

$$\mathbf{E} = \frac{m}{e} \mathbf{E}_g = \frac{m}{e} \mathbf{g}, \tag{79}$$

while the corresponding potential difference reads

$$\Delta V = \frac{m}{e} \Delta V_g = \int_0^\ell dz \frac{m}{e} g = \frac{m}{e} g \ell, \tag{80}$$

having chosen the z-axis along the direction of the gravitational field, see Figure 1. The resulting induced Josephson current [77] then has the form

$$I_s(t) = I_0 \sin\left(\frac{2e\Delta V}{\hbar}t + \varphi\right) = I_0 \sin(\omega t + \varphi). \tag{81}$$

We also expect the induced effect to disappear when the junction is rotated in a position where the normal vector to the surface is perpendicular to the gravitational field direction.

Experimental Settings

Let us first consider a junction involving high- T_c superconductors (HTSC). The latter have a coherence length ξ of the order of 10^{-9} m that fixes the thickness ℓ of the insulating layer to be $\ell \lesssim \xi$. Then, if we consider the pulsation

$$\omega = \frac{2e\Delta V}{\hbar} = \frac{2mg\ell}{\hbar}, \quad (82)$$

a junction with an insulating layer of thickness $\ell \simeq 1$ nm would result in $\omega \simeq 1.7 \times 10^{-4} \text{ s}^{-1}$, determining a corresponding period for the Josephson current $T = 2\pi/\omega \simeq 3.7 \times 10^4$ s. This implies that the distinctive oscillatory behaviour can be observed only in very stable junctions, since a reasonable duration of the experiment turns out to be longer than one day, see Figure 2.

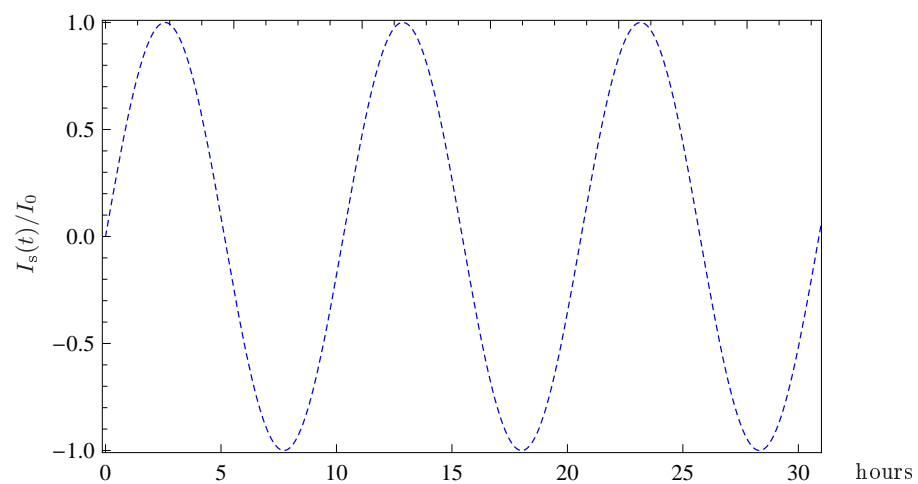


Figure 2. Time dependence of the Josephson current for an insulating layer of thickness $\ell = 1$ nm.

To reduce the time duration of the experiment, it is necessary to increase the voltage V_g . Clearly, it is impossible to vary the intensity of the local gravitational field, so that the only strategy left is to have larger ℓ . This means that we need tunnelling junctions working in the presence of a thicker insulating layer: this is possible using low- T_c superconductors (LTSC), and the latter can feature a larger coherent length, of the order of 10^3 nm. In this case, we can take an insulating layer of thickness $\ell \simeq 300$ nm and obtain for the voltage $V_g \simeq 1.67 \times 10^{-17}$ Volt. The pulsation turns out to be $\omega \simeq 0.05 \text{ s}^{-1}$ and the corresponding period $T \simeq 123$ s, strongly reducing the experiment duration, see Figure 3.

From a practical point of view, it would be preferable to work with experimental setups stable enough to allow accurate oscillations measurements, but that, at the same time, give rise to a Josephson current of detectable intensity. If we increase the junction thickness using low- T_c superconductors, the time duration for the experiment decreases and a stable setting is then possible, but the associated Josephson current becomes very weak and difficult to measure. Currently, the best choice to observe experimental evidence is to realize the most stable setup possible with HTCS, and then make long-time measurements of stronger Josephson currents.

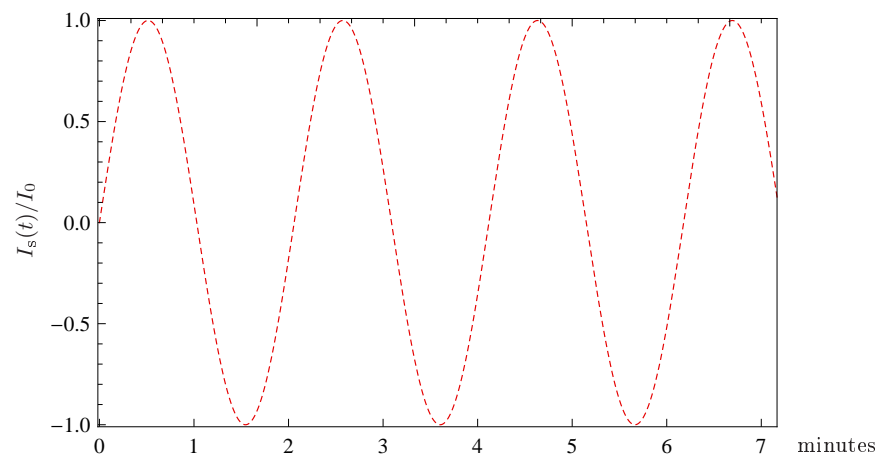


Figure 3. Time dependence of the Josephson current for an insulating layer of thickness $\ell = 300$ nm.

We have seen how the proposed theoretical model provides the possibility to investigate the discussed interplay between gravitation and a superconductive condensate. For the simple case of the Josephson junction, the difficulties lie in the experimental setup that has to be stable in time to allow for careful observations of the oscillatory behaviour, and very sensitive to the induced voltage. In the following sections, we are going to analyse a more detailed microscopic description of the superfluid, exploiting a mean-field theory formulation for the system thermodynamics, including the effects of thermal fluctuations. In particular, we will analyse how the local gravitational field can be affected by the presence of a supercondensate exploiting the time-dependent Ginzburg–Landau equations in the regime of fluctuations.

4. Affecting the Field Just Outside the Sample: Ginzburg–Landau Formulation

We now want to better characterize the interaction between the superfluid and the local gravitational field. To this end, we need a microscopic quantum model describing the supercondensate behaviour. However, the formalism that characterizes the material superconductive state is in general very complicated, so that extracting quantitative predictions (or even just qualitative descriptions) for the interplay turns out to be an almost impossible task.

A simpler framework for analysing the interaction mechanism is given by a superconducting sample in the vicinity of its critical temperature T_c . In particular, for T near T_c , the system can be described by the Ginzburg–Landau equations, for which analytic solutions could be found.

4.1. Thermodynamic Fluctuations vs. Mean-Field Theory

The physics of low-temperature condensed matter systems is based on two fundamental notions: the low-energy long-living excitations (quasiparticles) and the mean field approximation. For instance, the BCS theory of superconductivity [106] is a paradigmatic example of the exploitation of both approaches mentioned.

Physical situations which cannot be consistently described in terms of the quasiparticle method or the mean field approximation are called *fluctuations*. The regime in which the fluctuations come into play is, in general, a very narrow temperature range around the critical temperature (On the contrary, for high temperature cuprate superconductors, organic superconductors, iron pnictides, low dimensional and amorphous superconducting systems, the situation changes radically due to the very small value of the coherence length, so that the temperature range of fluctuation is considerably larger). In particular, many effects on the superconducting phase occur while the system is still in

the normal phase (just above the critical temperature) and originate from the appearance of the superconducting fluctuations themselves. In this regard, diamagnetic susceptibility, conductivity, heat capacity and other physical quantities may increase considerably near the transition temperature.

If we consider a range of temperature sufficiently far from the critical T_c , the fluctuation regime ceases and the physics of the system is described in terms of a mean field formulation. The latter approach approximates the physics by averaging over the degrees of freedom of the system, that is, by approximating all the interactions acting on a single component with a single averaged effect. The technique allows for map a multi-body problem onto a one-body problem. In particular, the thermodynamic properties of the system are obtained by treating the order parameter as spatially constant, the spatial fluctuations being negligible. Many predictions can therefore be obtained by exploiting a much simpler mathematical formulation: this is a great advantage when dealing with new and unconventional systems, for which a complete description is not known.

GL Equations

As we have briefly discussed, the analysis of condensed matter systems in general involves the study of complicated, many electron states. A certain number of phenomenological approaches, based on classical field theory, were then developed to address the problem. A possibility is to consider a slowly-varying density of fields, carrying sufficient quantum information to write down an energy function for the system to be minimized: this corresponds to the celebrated Ginzburg–Landau (GL) formulation [107,108], based on a mean field approach. Its most notable use is in the theory of superconductors, where a complex scalar field ψ is used to characterize the density of the superconducting paired electrons. Even if the GL approach is, in general, superseded by the more fundamental BCS theory, it is a powerful tool in the vicinity of the critical temperature, where a more fundamental theory is lacking or the formulation is too complicated.

4.2. Ginzburg–Landau Formulation

Let us consider a superconductive sample near its critical temperature. At the microscopic level, thermodynamic fluctuations of the order parameter $\psi(\mathbf{x}, t)$ describing superconducting electrons occur, giving rise to localized regions of accelerated charge carriers [109–113]. From a physical point of view, ψ can be thought as the pseudowavefunction characterizing the motion of the center of mass of the Cooper pairs. The average size of these regions is much greater than the mean free path for a certain range of temperature above T_c , while it decreases for larger temperature [114]. Moreover, we are going to consider sufficiently dirty materials, so that the effects of the fluctuations can be observed over a sizable range of temperature [111] (In order to have a sufficiently large temperature interval, the electronic mean free path characterizing the material in the normal state should be less than 10 Å).

We now want to characterize in more detail the behaviour of the superconductive sample, also analysing its possible interaction with the surrounding gravitational field. If the sample is put at a temperature T slightly greater than T_c but sufficiently far from the transition point (mean field regime), the system can be described in terms of linearized time-dependent Ginzburg–Landau equations (The order parameter being very small in the thermodynamic fluctuations regime, a linear order formulation can be exploited). The latter can be expressed in the gauge-invariant form as [115–117]:

$$\Gamma(\hbar \partial_t - 2ie\phi)\psi = \frac{1}{2m}(\hbar \nabla\phi - 2ie\mathbf{A})^2\psi + \alpha\psi \quad (T > T_c) . \quad (83)$$

where $\psi(\mathbf{x}, t)$ is the order parameter, $\phi(\mathbf{x}, t)$ the electric potential and $A(\mathbf{x}, t)$ is the vector potential. We also introduce the quantities:

$$\Gamma = \frac{\alpha}{\epsilon(T)} \frac{\pi}{8 k_B T_c} \quad \epsilon(T) = \sqrt{\frac{T - T_c}{T_c}} \quad \xi(T) = \frac{\xi_0}{\sqrt{\epsilon(T)}} \quad \alpha = \frac{\hbar^2}{2m \xi(T)^2} \quad (84)$$

ξ_0 being the BCS intrinsic coherence length, roughly characterizing the smallest size of a wave packet formed by superconducting charge carriers. It plays a role analogous to the mean free path in the nonlocal electrodynamics of normal metals and is in general larger in metal superconductors (In spite of the fact that the two electrons in a Cooper pair can be far apart from each other, other electrons belonging to different Cooper pairs are usually closer). The temperature-dependent Ginzburg–Landau coherence length $\xi(T)$ provides a measure of the distance over which the order parameter can vary without undue energy increase, for a given temperature T . Alternatively, it can be thought of as a characterization of the distance from the surface over which the order parameter is close to its bulk value.

We now consider the following ansatz for the solution:

$$\psi(\mathbf{x}, t) = f(\mathbf{x}, t) \exp(i g(\mathbf{x}, t)), \quad (85)$$

and obtain from (83) the relations

$$\Gamma \hbar \frac{\partial f}{\partial t} = \alpha f - \frac{1}{2} m v_s^2 f + \frac{\hbar^2}{2m} \Delta f, \quad (86a)$$

$$\Gamma \hbar f \frac{\partial g}{\partial t} = 2 e \Gamma \phi f - \frac{\hbar^2}{2m} f \Delta g - 2 \hbar \mathbf{v}_s \cdot \nabla f. \quad (86b)$$

The superfluid speed \mathbf{v}_s has the form

$$\mathbf{v}_s = \frac{1}{m} \left(\hbar \nabla g + 2 \frac{e}{c} \mathbf{A} \right), \quad (87)$$

and the associated supercurrent density \mathbf{j}_s reads

$$\mathbf{j}_s = -2 \frac{e}{m} |\psi|^2 \left(\hbar \nabla g + 2 \frac{e}{c} \mathbf{A} \right) = -2 e f^2 \mathbf{v}_s. \quad (88)$$

4.2.1. Thermodynamic Fluctuations

The presence of a thermal energy of the order of $\sim k_B T$ implies that the system could fluctuate in different low-lying states with a non-zero probability. Let us then use f_k to define the value of f for a fluctuation of the wave vector \mathbf{k} . The above (86) can be recast in the form

$$\Gamma \hbar \frac{\partial f_k}{\partial t} = \alpha f_k - \frac{\hbar^2}{2m} k^2 f_k - \frac{1}{2} m v_s^2 f_k, \quad (89a)$$

$$\frac{\partial \mathbf{v}_s}{\partial t} = -2 \frac{e}{m} \mathbf{E} \quad (89b)$$

having used Equations (87), (86b) and

$$\nabla \phi = -\mathbf{E} - \frac{\partial \mathbf{A}}{\partial t}. \quad (90)$$

Equation (89b) can be easily integrated and the resulting expression for the superfluid speed can be used in (89a) giving

$$\Gamma \hbar \frac{\partial f_k}{\partial t} = \left(\alpha - \frac{\hbar^2}{2m} k^2 - 2 \frac{e^2}{m} E^2 t^2 \right) f_k. \tag{91}$$

We then find for f_k

$$f_k(t) = f_k(0) \exp \left(\frac{\left(\alpha - \frac{\hbar^2}{2m} k^2 \right) t - \frac{2}{3} \frac{e^2}{m} E^2 t^3}{\Gamma \hbar} \right), \tag{92}$$

with

$$f_k^2(0) = \frac{k_B T}{2 \left(|\alpha| + \frac{\hbar^2}{2m} k^2 \right)}, \tag{93}$$

and the associated current density $\mathbf{j}_{sk}(t)$ can be written as

$$\mathbf{j}_{sk}(t) = \frac{4e^2}{m} \mathbf{E} t f_k^2(0) \exp \left(2 \frac{\left(\alpha - \frac{\hbar^2}{2m} k^2 \right) t - \frac{2}{3} \frac{e^2}{m} E^2 t^3}{\Gamma \hbar} \right). \tag{94}$$

Finally, the explicit expression for the physical supercurrent density \mathbf{j}_s [76] can be found integrating over \mathbf{k} :

$$\mathbf{j}_s(t) = \frac{1}{8\pi^3} \int_0^{+\infty} dk 4\pi k^2 \mathbf{j}_{sk}(k, t), \tag{95}$$

where we have considered a three-dimensional sample of dirty material, whose dimensions are larger than the correlation length.

4.2.2. Generalized EM Fields

The above expression for the supercurrent density allows for extracting the explicit form of the generalized electromagnetic fields and potentials characterizing the physical evolution of the system. First of all, the vector potential $\mathbf{A}(x, y, z, t)$ is obtained from

$$\mathbf{A}(x, y, z, t) = \frac{\mu_0}{4\pi} \int \frac{\mathbf{j}_s(t') dx' dy' dz'}{\sqrt{(x-x')^2 + (y-y')^2 + (z-z')^2}}, \tag{96}$$

where t' is the retarded time

$$t' = t - \frac{\sqrt{(x-x')^2 + (y-y')^2 + (z-z')^2}}{c}. \tag{97}$$

The generalized electric field $\mathbf{E}(x, y, z, t)$ (39) is obtained from:

$$\mathbf{E}(x, y, z, t) = -\frac{\partial \mathbf{A}(x, y, z, t)}{\partial t} + \frac{m}{e} \mathbf{g}. \tag{98}$$

As we can appreciate, the generalized gravito–Maxwell $\mathbf{E}(x, y, z, t)$ features two contributions. In particular, the second term is the standard, constant weak Earth’s gravity contribution. On the other hand, the unconventional first term originates from the presence of the (non-constant) supercurrent density and can determine a local, additional contribution to the constant gravitational field \mathbf{g} . The final result clearly depends on the superconducting sample shape and dimensions, as well as on the space point (outside the sample) where the gravitational fluctuation is measured.

4.3. Expected Effects

Let us now study in detail a suitable experimental setting to evaluate the proposed interplay. Here, we consider a superconductive disk at a temperature higher but very close to T_c . The sample is kept in the normal state by a weak magnetic field that is then turned off at the time $t = 0$, where the superconductive transition occurs. The axis of the disk is aligned with the direction of the gravitational field, the bases being parallel to the ground.

The chosen temperature regime ($T \gtrsim T_c$) corresponds to the thermodynamic fluctuations regime we discussed in the previous section, so that we can exploit the corresponding results for the supercurrent and generalized EM fields expressions, see Equations (95), (96) and (98). We are interested in the gravitational correction along the axis of the disk, just above the upper base of cylindrical sample.

First, we consider the local alteration of the gravitational as a function of time. In Figure 4, we show the computed effect for an In sample. The latter is a low- T_c metallic superconductor, then featuring a large intrinsic coherence length ξ_0 . The same analysis is then performed in Figure 5 for a $\text{Ba}_{0.4}\text{K}_{0.6}\text{Fe}_2\text{As}_2$ sample, an high- T_c superconductor with small ξ_0 . In both cases, the variation is measured along the disk axis, at a fixed distance d above the base surface. We can note that the local gravitational field is initially reduced with respect to the unperturbed value; then, it increases up to a maximum $g + \Delta$ for $t = \tau_0$ and it finally relaxes to the standard unperturbed value g (We can also note that, for a very short time interval, the local field seems to change sign: this can be prevented by means of appropriate physical cutoffs, excluding the arbitrary growth of instabilities which would give rise to negative values [8]).

We then focus on the local alteration as a function of the distance from the sample for fixed time. In particular, we choose to maximize the effect putting ourselves at $t = \tau_0$. In Figures 6 and 7, it is shown the variation, measured along the axis of the disk above the base surface, for the same In and $\text{Ba}_{0.4}\text{K}_{0.6}\text{Fe}_2\text{As}_2$ samples. In both cases, the effect is stronger in the vicinity of the sample, as it seems reasonable.

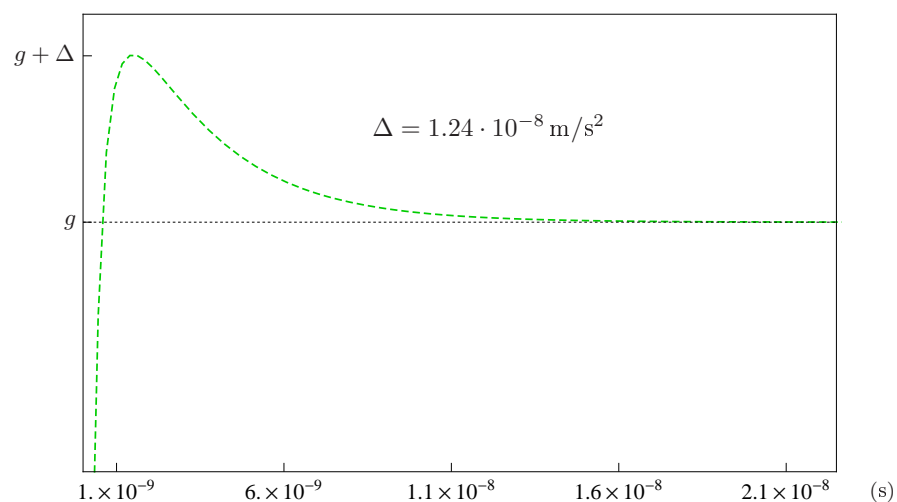


Figure 4. Local gravitational field variation as a function of time for a In sample ($\xi_0 = 360$ nm, $T_c = 3.410$ K, $\Delta T = 10^{-3}$ K [118]) measured along the axis of a superconductive disk at fixed distance $d = 0.1$ cm above the base surface. The disk radius is $R = 15$ cm and the disk thickness is $h = 3$ cm.

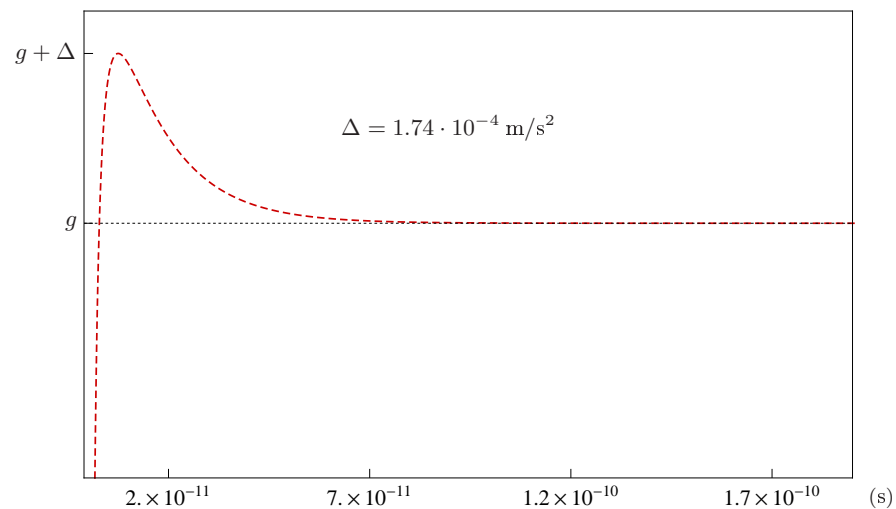


Figure 5. Local gravitational field variation as a function of time for a $\text{Ba}_{0.4}\text{K}_{0.6}\text{Fe}_2\text{As}_2$ sample ($\xi_0 = 1.20$ nm, $T_c = 37.0$ K, $\Delta T = 0.1$ K [119]) measured along the axis of a superconductive disk at fixed distance $d = 0.1$ cm above the base surface. The disk radius is $R = 15$ cm and the disk thickness is $h = 3$ cm.

From a preliminary qualitative analysis, it is possible to show that the maximum perturbation value Δ of the local field is proportional to inverse of the coherence length,

$$\Delta \propto \zeta(T)^{-1}. \quad (99)$$

This suggests that a stronger affection can be obtained by using high- T_c superconductors (the latter featuring smaller coherence length) and can be appreciated comparing the strength of the perturbation for low and high- T_c superconducting samples in the presented Figures.

On the other hand, it is easily demonstrated that the maximal effect occurs after a time interval

$$\tau_0 \propto (T - T_c)^{-1}. \quad (100)$$

This means that the time range in which the perturbation takes place can be extended keeping the sample at a temperature close to the transition temperature. From this point of view, if we want to be very close to the effective critical T_c , it could be easier to consider a low- T_c sample, the temperature transition range being very narrow for the latter. However, this in turns results in a reduced alteration of the local field, since, close to T_c , the Ginzburg–Landau coherence length $\zeta(T)$ diverges, see Equation (84).

In light of the above discussion, an optimized experimental settings should involve a large high- T_c superconducting sample at a temperature very close to T_c . The latter condition could help in extending the time range in which the effect takes place, while choosing a high- T_c superconductor would determine an enhanced local alteration due to the short intrinsic coherence length. Finally, large dimensions for the sample give a larger integration range and a resulting stronger contribution.

The above considerations show how a careful arrangement of the experimental setup is very important, since the material parameters and the sample geometry, dimensions and temperature directly affect the magnitude of the interaction and the related time scales. In this regard, the very short time intervals in which the effect occurs complicate direct measurements.

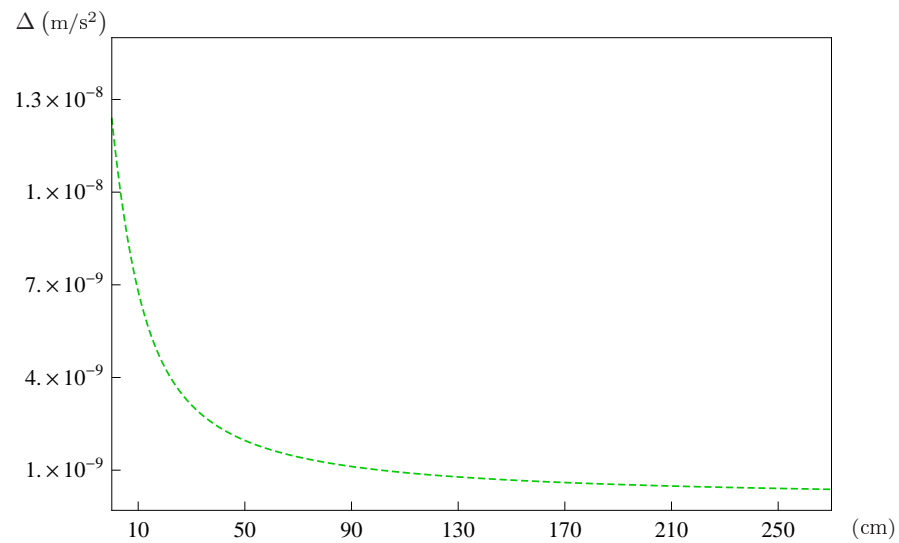


Figure 6. Local gravitational field variation as a function of distance for the same In sample, measured along the disk axis above the base surface, at fixed time $t = \tau_0 = 1.64$ ns. The disk radius is $R = 15$ cm and the disk thickness is $h = 3$ cm.

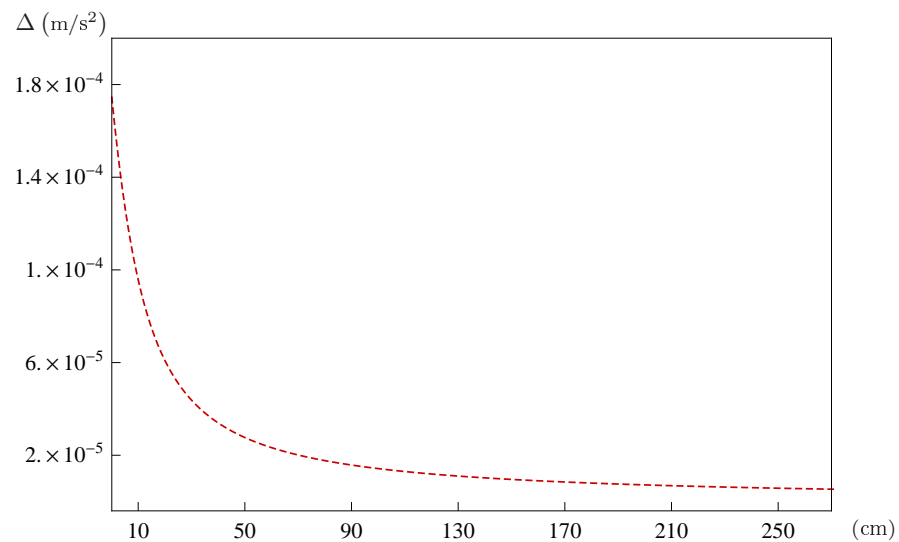


Figure 7. Local gravitational field variation as a function of distance for the same $\text{Ba}_{0.4}\text{K}_{0.6}\text{Fe}_2\text{As}_2$ sample, measured along the disk axis above the base surface at fixed time $t = \tau_0 = 7.50 \times 10^{-3}$ ns. The disk radius is $R = 15$ cm and the disk thickness is $h = 3$ cm.

In the following chapter, we will consider the possible affection of the local gravitational field in the sample interior exploiting again the effective framework of the gravito–Maxwell formulation combined with the Ginzburg–Landau formalism. The analysis will suggest that, in the superfluid region, a slight affection of the local field could take place, as we have discussed in Section 1 considering the formal quantum gravity point of view. A possibility to enhance the effect comes from the presence of suitable electric and magnetic fields, determining the formation of moving vortices and giving rise to a further interaction with the local gravitational field.

5. Affecting the Field Inside the Sample: Vortex Lattice

Now, we want to consider the possible alteration of the local static gravitational field in the region inside the superfluid. To this end, we will exploit the time-dependent Ginzburg–Landau equations for the supercondensate order parameter, looking for analytic

solutions in the weak field condition. First, we will restrict to the simpler case of an isolated isotropic superconductor immersed in the Earth’s gravity in the absence of external EM fields. Then, we will analyse a more complicated setup, switching on suitable electric and magnetic fields: this will give rise to the formation of a vortex lattice inside the superfluid, possibly determining stronger effects for the proposed interplay.

5.1. Time-Dependent Ginzburg–Landau Formulation

Let us consider the case of a superconducting sample on the Earth surface. We already pointed out that the situation leads to the appearance of effective, generalized Maxwell fields. In particular, the local static weak gravitational field is treated as the gravitational component of the generalized gravitoelectric field, exploiting the formal analogy discussed in the previous Section 2.

The chosen physical system can be characterized in terms of time-dependent Ginzburg–Landau equations (TDGL). The latter are derived minimizing the total Gibbs free energy of the system [92–94], and can be written in a general explicit form as [120–126]:

$$\frac{\hbar^2}{2m} \left(i \nabla + \frac{2e}{\hbar} \mathbf{A} \right)^2 \psi - a \psi + b |\psi|^2 \psi = - \frac{\hbar^2}{2m \mathcal{D}} \left(\frac{\partial}{\partial t} + \frac{2ie}{\hbar} \phi \right) \psi, \tag{101a}$$

$$\nabla \times \nabla \times \mathbf{A} - \nabla \times \mathbf{B} = \mu_0 (\mathbf{j}_n + \mathbf{j}_s) \tag{101b}$$

where \mathbf{j}_n and \mathbf{j}_s are expressed as

$$\mathbf{j}_n = -\sigma \left(\frac{\partial \mathbf{A}}{\partial t} + \nabla \phi \right), \tag{102}$$

$$\mathbf{j}_s = -i \hbar \frac{e}{m} (\psi^* \nabla \psi - \psi \nabla \psi^*) - \frac{4e^2}{m} |\psi|^2 \mathbf{A}.$$

and correspond to the contributions of the normal current and supercurrent densities, respectively. In the above expressions, σ is the conductivity in the normal phase, \mathcal{D} is the diffusion coefficient, \mathbf{B} is the applied field, and the vector potential \mathbf{A} is minimally coupled to ψ . The coefficients a and b in (101a) can be written as:

$$a = a(T) = a_0 (T - T_c) \qquad b = b(T_c) \tag{103}$$

where is T_c the critical temperature of the superconductor, while a_0 and b are positive constant quantities. We can write consistent boundary and initial conditions for the system as

$$\left. \begin{aligned} \left(i \nabla \psi + \frac{2e}{\hbar} \mathbf{A} \psi \right) \cdot \mathbf{n} &= 0 \\ \nabla \times \mathbf{A} \cdot \mathbf{n} &= \mathbf{B} \cdot \mathbf{n} \\ \mathbf{A} \cdot \mathbf{n} &= 0 \end{aligned} \right\} \text{on } \partial\Omega \times (0, t), \qquad \left. \begin{aligned} \psi(x, 0) &= \psi_0(x) \\ \mathbf{A}(x, 0) &= \mathbf{A}_0(x) \end{aligned} \right\} \text{on } \Omega, \tag{104}$$

where $\partial\Omega$ is the boundary of a smooth and simply connected domain in \mathbb{R}^N .

Dimensionless TDGL

The above Equations (101) can be recast in a useful dimensionless form. To this end, we define the following quantities:

$$\begin{aligned} \Psi^2(T) &= \frac{|a(T)|}{b} & \zeta(T) &= \frac{\hbar}{\sqrt{2m|a(T)|}} & \lambda(T) &= \sqrt{\frac{bm}{4\mu_0|a(T)|e^2}} & \kappa &= \frac{\lambda(T)}{\zeta(T)} \\ \tau(T) &= \frac{\lambda^2(T)}{\mathcal{D}} & \eta &= \mu_0\sigma\mathcal{D} & B_c(T) &= \sqrt{\frac{\mu_0|a(T)|^2}{b}} = \frac{\hbar}{2\sqrt{2}e\lambda(T)\zeta(T)} \end{aligned} \tag{105}$$

where $\lambda(T)$, $\zeta(T)$ and $B_c(T)$ are the penetration depth, coherence length and thermodynamic critical field, respectively. We also introduce the dimensionless quantities

$$t' = \frac{t}{\tau} \quad x' = \frac{x}{\lambda} \quad y' = \frac{y}{\lambda} \quad \psi' = \frac{\psi}{\Psi} \tag{106}$$

and the new dimensionless fields and currents

$$\mathbf{A}' = \frac{\mathbf{A}\kappa}{\sqrt{2}B_c\lambda} \quad \phi' = \frac{\phi\kappa}{\sqrt{2}B_c\mathcal{D}} \quad \mathbf{E}' = \frac{\mathbf{E}\lambda\kappa}{\sqrt{2}B_c\mathcal{D}} \quad \mathbf{B}' = \frac{\mathbf{B}\kappa}{\sqrt{2}B_c} \quad \mathbf{j}' = \frac{\mathbf{j}\mu_0\lambda\kappa}{\sqrt{2}B_c} \tag{107}$$

We then insert the above Equations (106) and (107) in Equations (101) (we also drop the primes for the sake of notational simplicity) and get the dimensionless TDGL equations in a bounded, smooth and simply connected domain in \mathbb{R}^N [121,123]:

$$\frac{\partial\psi}{\partial t} + i\phi\psi + \kappa^2(|\psi|^2 - 1)\psi + (i\nabla + \mathbf{A})^2\psi = 0, \tag{108a}$$

$$\nabla \times \nabla \times \mathbf{A} - \nabla \times \mathbf{B} = \mathbf{j}_n + \mathbf{j}_s = -\eta \left(\frac{\partial\mathbf{A}}{\partial t} + \nabla\phi \right) - \frac{i}{2}(\psi^*\nabla\psi - \psi\nabla\psi^*) - |\psi|^2\mathbf{A}, \tag{108b}$$

while the boundary and initial conditions (104) in the dimensionless form read

$$\left. \begin{aligned} (i\nabla\psi + \mathbf{A}\psi) \cdot \mathbf{n} &= 0 \\ \nabla \times \mathbf{A} \cdot \mathbf{n} &= \mathbf{B} \cdot \mathbf{n} \\ \mathbf{A} \cdot \mathbf{n} &= 0 \end{aligned} \right\} \text{on } \partial\Omega \times (0, t); \quad \left. \begin{aligned} \psi(x, 0) &= \psi_0(x) \\ \mathbf{A}(x, 0) &= \mathbf{A}_0(x) \end{aligned} \right\} \text{on } \Omega. \tag{109}$$

5.2. Isolated Superconductor in the Weak Gravitational Field

Let us now try to solve the above equations for a superconductor immersed in the Earth’s static gravity in the absence of external electromagnetic fields (39):

$$\mathbf{E}_e = 0 \quad \mathbf{B}_e = 0 \quad \implies \quad \mathbf{E} = \frac{m}{e} \mathbf{E}_g \quad \mathbf{B} = 0 \tag{110}$$

having also set to zero the \mathbf{B}_g contribution that is negligible in the Solar system [28,127].

5.2.1. Solving TDGL Equations

A convenient gauge choice for subsequent calculations turns out to be $\phi = 0$, i.e., the vanishing of the scalar potential (Clearly, any alternative gauge shall not influence any physical results, the equations being gauge-invariant). From a physical point of view, this choice also reflects the absence of localized charges inside the superfluid, while

contributions to the total gravitational field originating from the sample mass are clearly totally irrelevant. The dimensionless TDGL then explicitly read [128]:

$$\frac{\partial \psi}{\partial t} = -(i \nabla + \mathbf{A})^2 \psi - \kappa^2 (|\psi|^2 - 1) \psi, \tag{111a}$$

$$\eta \frac{\partial \mathbf{A}}{\partial t} = -\nabla \times \nabla \times \mathbf{A} + \nabla \times \mathbf{B} - |\psi|^2 (\mathbf{A} - \nabla \theta) \tag{111b}$$

where $\psi \equiv \psi(\mathbf{x}, t)$ is a complex function that we can write as

$$\psi = |\psi| \exp(i\theta) = \text{Re } \psi + i \text{Im } \psi = \psi_1 + i \psi_2, \tag{112}$$

so that (111a) splits into two distinct equations for the real and imaginary parts ψ_1 and ψ_2 .

Let us now restrict to a one-dimensional field configuration, so that one has

$$\nabla \rightarrow \partial/\partial x \quad \mathbf{A} \rightarrow A_x \equiv A. \tag{113}$$

In this simplified framework, (111) reads:

$$\frac{\partial \psi_1}{\partial t} = \frac{\partial^2 \psi_1}{\partial x^2} + A \frac{\partial \psi_2}{\partial x} + \psi_2 \frac{\partial A}{\partial x} - \psi_1 A^2 - \kappa^2 (|\psi_1|^2 + |\psi_2|^2 - 1) \psi_1,$$

$$\frac{\partial \psi_2}{\partial t} = \frac{\partial^2 \psi_2}{\partial x^2} - A \frac{\partial \psi_1}{\partial x} - \psi_1 \frac{\partial A}{\partial x} - \psi_2 A^2 - \kappa^2 (|\psi_1|^2 + |\psi_2|^2 - 1) \psi_2, \tag{114}$$

$$\eta \frac{\partial A}{\partial t} = -\left(\psi_2 \frac{\partial \psi_1}{\partial x} - \psi_1 \frac{\partial \psi_2}{\partial x}\right) - (\psi_1^2 + \psi_2^2) A,$$

since, in one dimension, $\nabla^2 A = \frac{\partial}{\partial x} (\nabla \cdot \mathbf{A})$ and then

$$\nabla \times \nabla \times \mathbf{A} = \nabla (\nabla \cdot \mathbf{A}) - \nabla^2 A \stackrel{1d}{=} 0. \tag{115}$$

Then, let us consider an ideal, half-infinite superconductive region, see Figure 8. The \vec{u}_x direction is orthogonal to the superconducting separation surface, corresponding to the yz plane and parallel to the ground, so that, for $x > 0$, we find an empty space, while the superfluid region is located at $x \leq 0$. The whole setting is immersed in the Earth’s uniform and static gravitational field that is captured by the gravitoelectric component

$$\mathbf{E}_g^{\text{EXT}} = -g \vec{u}_x, \tag{116}$$

g being the standard gravity acceleration.

The *dimensional* form of the gravitoelectric field *inside* the superfluid region

$$\mathbf{E}_g = -\frac{\partial \mathbf{A}_g(t)}{\partial t}, \tag{117}$$

while (116) suggests for the external (*outside*) gravitational vector potential the form

$$\mathbf{A}_g^{\text{EXT}}(t) = g(C + t) \vec{u}_x, \tag{118}$$

C being a constant.



Figure 8. Half-infinite superconductor approximation. The Earth’s gravitational field is parallel to the \vec{u}_x direction.

In the 1D setup, the generalized external potential in the *dimensionless* form reads

$$A^{\text{EXT}} = \frac{m}{e} A_{\text{g}}^{\text{EXT}} \frac{\kappa}{\sqrt{2} B_C \lambda} = g_{\star} (c_1 + t), \quad (119)$$

where we have dropped the primes for notational simplicity. Using (105), we can also explicitly write

$$c_1 = \frac{C}{\tau}, \quad g_{\star} = \frac{m \kappa \lambda(T) g}{\sqrt{2} e \mathcal{D} B_C(T)} \ll 1. \quad (120)$$

Next, we express ψ_1 , ψ_2 and A as:

$$\psi_1(x, t) = \psi_{10}(x) + g_{\star} \gamma_1(x, t), \quad (121a)$$

$$\psi_2(x, t) = \psi_{20}(x) + g_{\star} \gamma_2(x, t), \quad (121b)$$

$$A(x, t) = g_{\star} \beta(x, t), \quad (121c)$$

where ψ_{10} and ψ_{20} characterize the unperturbed system and satisfy

$$0 = \frac{1}{\kappa^2} \frac{\partial^2 \psi_{10}}{\partial x^2} + \psi_{10} - \psi_{10} (\psi_{10}^2 + \psi_{20}^2), \quad (122a)$$

$$0 = \frac{1}{\kappa^2} \frac{\partial^2 \psi_{20}}{\partial x^2} + \psi_{20} - \psi_{20} (\psi_{10}^2 + \psi_{20}^2). \quad (122b)$$

the ψ_{10} and ψ_{20} behaviour therefore being described by equations of the same type.

We now choose to set

$$\psi_{20} = 0 \quad \Rightarrow \quad \psi_0 = \psi_{10} + i \psi_{20} = \psi_{10} \in \mathbb{R}, \quad (123)$$

so that (122a) reads

$$0 = \frac{1}{\kappa^2} \frac{\partial^2 \psi_{10}}{\partial x^2} + \psi_{10} - \psi_{10}^3, \quad (124)$$

and is solved by [94]

$$\psi_{10} = \tanh\left(\frac{\kappa x}{\sqrt{2}}\right). \quad (125)$$

We are therefore left with the following set of equations:

$$\frac{\partial \gamma_1}{\partial t} = \frac{\partial^2 \gamma_1}{\partial x^2} + \kappa^2 (1 - 3 \psi_{10}^2) \gamma_1, \tag{126a}$$

$$\frac{\partial \gamma_2}{\partial t} = \frac{\partial^2 \gamma_2}{\partial x^2} + \kappa^2 (1 - 3 \psi_{10}^2) \gamma_2 - \beta \frac{\partial \psi_{10}}{\partial x} - \psi_{10} \frac{\partial \beta}{\partial x}, \tag{126b}$$

$$\eta \frac{\partial \beta}{\partial t} = - \left(\gamma_2 \frac{\partial \psi_{10}}{\partial x} - \psi_{10} \frac{\partial \gamma_2}{\partial x} \right) - \psi_{10}^2 \beta, \tag{126c}$$

the last (126c) implying that $\beta(x, t)$ does not depend on $\gamma_1(x, t)$.

If we now decide to put ourselves away from borders, we can set $\psi_{10} \simeq 1$ in (126), resulting in

$$\frac{\partial \gamma_1}{\partial t} \simeq \frac{\partial^2 \gamma_1}{\partial x^2} - 2 \kappa^2 \gamma_1, \tag{127a}$$

$$\frac{\partial \gamma_2}{\partial t} \simeq \frac{\partial^2 \gamma_2}{\partial x^2} - 2 \kappa^2 \gamma_2 - \frac{\partial \beta}{\partial x}, \tag{127b}$$

$$\eta \frac{\partial \beta}{\partial t} \simeq \frac{\partial \gamma_2}{\partial x} - \beta. \tag{127c}$$

We then find for β the solution

$$\beta(x, t) = e^{-\frac{t}{\eta}} \left(b_1(x) + \frac{1}{\eta} \int_0^t dt e^{\frac{t}{\eta}} \frac{\partial \gamma_2(x, t)}{\partial x} \right). \tag{128}$$

where $b_1(x) = c_1$, as it is implied by Equation (121c) for $t \rightarrow 0$.

Let us imagine that the sample transition to the superconducting state occurs at $t = 0$. We also make the natural assumption that, before the transition, no alteration of the gravitational field takes place (material in the normal state), the gravitational field assuming the same value inside and outside the sample region for $t < 0$. This results in the following boundary and initial conditions:

$$\begin{aligned} \psi(0, t) = 0 & \quad \psi(x, 0) = \psi_{10}(x) & \quad \frac{\partial \psi_1}{\partial x}(x, 0) = 0 \\ \gamma_1(0, t) = 0 & \quad \gamma_1(x, 0) = 0 & \quad \frac{\partial \gamma_1}{\partial x}(x, 0) = 0 \\ \gamma_2(0, t) = 0 & \quad \gamma_2(x, 0) = 0 & \quad \frac{\partial \gamma_2}{\partial x}(x, 0) = 0 \end{aligned} \tag{129}$$

together with the condition for β

$$\lim_{t \rightarrow 0} g_\star \frac{\partial \beta}{\partial t}(x, t) = g_\star. \tag{130}$$

implying that the interplay occurs only in the presence of a superconducting phase.

In order to fix the dimensionless constant c_1 , we use Equations (117), (121c) and (126c) to write the relation between E_g and β as

$$\frac{E_g}{g_\star} = - \frac{\partial \beta}{\partial t} = \frac{1}{\eta} \left(\gamma_2 \frac{\partial \psi_{10}}{\partial x} - \psi_{10} \frac{\partial \gamma_2}{\partial x} \right) + \frac{\psi_{10}^2}{\eta} \beta. \tag{131}$$

To satisfy the hypothesis that any affection of the gravitational field occurs only after the appearance of a superconducting phase ($t > 0$), we assume

$$\lim_{t \rightarrow 0^-} \frac{E_g}{g_\star} = 1, \tag{132}$$

while, from the initial conditions in (129), we also have

$$\lim_{t \rightarrow 0} \gamma_2(x, t) = 0 \quad \lim_{t \rightarrow 0} \frac{\partial \gamma_2}{\partial x}(x, t) = 0. \tag{133}$$

We then obtain

$$t \rightarrow 0: \quad 1 = \frac{\psi_{10}^2}{\eta} \beta(x, 0) = \frac{\psi_{10}^2}{\eta} \frac{A^{\text{EXT}}(0)}{g_\star} = \frac{\psi_{10}^2}{\eta} c_1 \implies c_1 = \frac{\eta}{\psi_{10}^2}. \tag{134}$$

This c_1 constant is ineffective in empty space, while it is responsible for the desired, unconventional effects in the presence of the superconductor.

Finally, we can write the final form for $\beta(x, t)$ away from borders ($\psi_{10} \simeq 1, c_1 \simeq \eta$):

$$\beta(x, t) = e^{-\frac{t}{\eta}} \left(\eta + \frac{1}{\eta} \int_0^t dt e^{\frac{t}{\eta}} \frac{\partial \gamma_2(x, t)}{\partial x} \right), \tag{135}$$

from which we obtain the ratio

$$\frac{E_g}{g_\star} = -\frac{\partial \beta(x, t)}{\partial t} = \frac{1}{\eta} e^{-\frac{t}{\eta}} \left(\eta + \frac{1}{\eta} \int_0^t dt e^{\frac{t}{\eta}} \frac{\partial \gamma_2(x, t)}{\partial x} \right) - \frac{1}{\eta} \frac{\partial \gamma_2(x, t)}{\partial x}. \tag{136}$$

The discussed formulation characterizes more explicitly the proposed interplay between gravity and supercondensates in the presented, simplified setup. First, we see that the external gravitational vector potential seems to play a role in the superconducting transition: in particular, the external constant c_1 tends to assume fixed values depending on the specific properties of the sample undergoing the superconducting transition. On the other hand, we expect the back-reaction on the local gravitational to take place only after the transition itself, when the vector potential begins to “perceive” the presence of a superfluid phase.

5.2.2. Expected Effects

The above (136) for the ratio E_g/g_\star can be used to estimate the value of gravitational field inside the superconductor just after the superconducting phase transition:

$$t \simeq 0^+ : \quad \frac{E_g}{g_\star} \simeq 1 - \frac{t}{\eta} - \frac{1}{\eta} \frac{\partial \gamma_2(x, 0^+)}{\partial x}. \tag{137}$$

In the superconducting state, the alteration of the local field depends on physical characteristic of the involved sample. In particular, (137) shows that the relevant quantities are η , and the spatial derivative of γ_2 .

In order to enhance the interaction, we should maximize the variation $\frac{\partial \gamma_2}{\partial x}$, an effect than can be achieved by introducing suitable disorder in the material sample (This can be obtained, for instance, by means of chemical doping or proton irradiation). A maximized effect would also require small values for η . The latter is proportional to the product of the diffusion coefficient \mathcal{D} times the conductivity just above T_c , see (105). This would suggest to consider materials that are bad conductors in the normal state and have low Fermi energies (for example, cuprates).

Finally, we have to take into account the (usually very small) time scales in which the effect occurs, expressed by the τ coefficient

$$\tau(T) = \frac{\lambda^2(T)}{\mathcal{D}} \quad \text{with} \quad \lambda(T) \simeq \frac{\lambda_0}{\sqrt{\frac{T_c - T}{T_c}}} \tag{138}$$

The latter can be maximized with a reduced diffusion coefficient and large penetration length, as occurs in superconducting cuprates with internal disorder.

Performing measurements at a temperature close to T_c would give rise to enhanced effects: for example, in the case of $\text{Bi}_2\text{Sr}_2\text{CaCu}_2\text{O}_8$ ($T_c \simeq 109\text{ K}$, $\lambda_0 \simeq 500\text{ nm}$, $\sigma^{-1} \simeq 3.6 \times 10^{-6}\ \Omega\text{ m}$, $\mathcal{D} \simeq 10^{-3}\text{ m}^2/\text{s}$, $\xi_0 \simeq 1.4\text{ nm}$ [118]) for $T \simeq 105\text{ K}$, we find

$$T \simeq 105\text{ K} : \quad \tau \simeq 6.8 \times 10^{-9} \quad \eta \simeq 3.5 \times 10^{-4} \tag{139}$$

This would determine a reduction of the local gravitational field of the order of 2×10^{-5} , see Equation (137) neglecting the last term (Non-irradiated high- T_c superconductors (like BSCCO) usually feature low disorder, resulting in reduced values for the spatial derivative of γ_2).

The above analysis shows how a perceptible affection of the local field inside the sample is possible even in a simplified setup (zero EM fields). Experimental difficulties may still arise from the short time intervals in which the effect manifests itself (see the previous Section 4.3). In addition, in this case, an appropriate choice of the material parameters is essential, in order to enhance the interaction and extend the time ranges to workable scales.

In the following section, we will analyse a more complicated setup involving external electric and magnetic fields, which in turn determine the presence of moving vortices. The new configuration will not only result in an additional affection of the local gravitational field, but also in the appearance of a new component of the generalized electric field inside the sample, parallel to the superconductor surface.

5.3. Switching on EM Fields: Vortex Lattice

We now consider a superconducting sample with finite thickness L and very large dimensions along \vec{u}_z and \vec{u}_y directions. The sample is immersed in an external magnetic field \mathbf{B}_0 and has a square lattice of vortices, whose axes are directed along \mathbf{B}_0 . We choose the latter as

$$\mathbf{B}_0 = B_0 \vec{u}_z, \tag{140}$$

together with a vector potential \mathbf{A} of the form

$$\mathbf{A} = B_0 x \vec{u}_y. \tag{141}$$

Here, we decide to work in the Coulomb gauge $\nabla \cdot \mathbf{A} = 0$, where

$$\nabla^2 \mathbf{A} = -\mu_0(\mathbf{j}_n + \mathbf{j}_s). \tag{142}$$

We also allow for the presence of a constant external (standard) electric field $\mathbf{E}_0^{(e)}$ along the \vec{u}_x direction. Given the simultaneous presence of the Earth’s static gravity, the situation gives rise to a *generalized* static field \mathbf{E}_0 of the form

$$\mathbf{E}_0 = \mathbf{E}_0^{(e)} + \mathbf{E}_0^{(g)} = \left(E_0^{(e)} - E_0^{(g)} \right) \vec{u}_x = \left(E_0^{(e)} - \frac{m}{e} g \right) \vec{u}_x = E_0 \vec{u}_x, \tag{143}$$

and a related scalar potential

$$\phi_0 = -E_0 x. \tag{144}$$

As in the previous case, the transition takes place at $t = 0$. In particular, for $t < 0$, we also have $T < T_c$ and $B > B_{c2}$, while, at $t = 0$, we still have $T < T_c$ but $B \simeq B_{c2}$. The external vector potential (outside the superfluid) is denoted by \mathbf{A}_0 , and coincides with the inside value for $t < 0$ (sample in the normal state and very weakly diamagnetic material).

5.3.1. Linearized TDGL

In the new setup with non-zero external EM fields, it is possible to write an analytic approximate solution of the TDGL (101) for the order parameter as

$$\psi(x, y, t) = \sum_{n=-\infty}^{\infty} c_n \exp\left(i q n \left(y + \frac{E_0}{B_0} t\right)\right) \exp\left(-\frac{1}{2 \xi(T)} \left(x - \frac{\hbar q n}{2 e B_0}\right)^2 + i \frac{e E_0 \xi^2(T)}{\hbar D} \left(x - \frac{\hbar q n}{2 e B_0}\right)\right). \tag{145}$$

The expression is valid for an external magnetic field $B_0 \lesssim B_{c2}$ and is then a solution of linearized TDGL equations [129,130] describing the behaviour of an ordered vortex lattice, moving under the influence of the external E_0 .

The above solution does not necessarily hold for different values of the magnetic field (for instance, $B_0 \sim B_{c1}$), where the order parameter values are bigger and the linearized approximation does not hold. Moreover, close to B_{c2} , the vortices are densely packed and the distance between them can be estimated to be of the order the coherence length $\xi(T)$. This can be then used to precisely characterize the vortex lattice, while this is not possible for generic values of B_0 [94]. (The presence of the external electric fields causes vortices motion and determines dissipative phenomena even in the superconducting state; it is possible to prevent it and anchor the vortices (vortex pinning) by introducing defects in the sample, thus reducing or eliminating energy dissipation [129]).

From an experimental point of view, in high- T_c superconductors, the formation of a square lattice seems to be energetically favourable, and, in the following, we will restrict to this possibility (This is not the case for low- T_c superconductors, where a triangular lattice formation usually occurs). We denote by q the distance between adjacent vortices that, for a square lattice, reads [131]

$$q \simeq \frac{2\pi}{\xi(T)}, \tag{146}$$

and the general c_n coefficients could be replaced by the correspondent c_{\square} expression for the square lattice:

$$c_n \rightarrow c_{\square} = \frac{2\sqrt{2}\pi}{\xi^2(T)}, \tag{147}$$

the c_{\square} coefficients being then independent of n .

5.3.2. Dimensionless Framework

Let us now consider the useful introduced dimensionless formulation. Working in the dimensionless version of the chosen Coulomb gauge $\nabla' \cdot \mathbf{A}' = 0$ it is possible to write a first-order expression for the dimensionless order parameter satisfying a linearized form for adimensional TDGL Equation (108) as [132]:

$$\psi(x, y, t) = \sum_{n=-\infty}^{\infty} |c_n| \exp\left(i q n \left(y + \frac{E_0}{B_0} t\right)\right) \exp\left(-\frac{\kappa^2}{2} (x - n x_0)^2 + i \frac{E_0}{\kappa} (x - n x_0)\right), \tag{148}$$

with

$$|\psi|^2 = \sum_{n=-\infty}^{\infty} |c_n|^2 \exp\left(-\kappa^2 (x - n x_0)^2\right). \tag{149}$$

The equations for the vector potential components read

$$\begin{aligned} \frac{\partial^2 A_x(x,t)}{\partial x^2} &= \eta \left(\frac{\partial A_x(x,t)}{\partial t} - E_0 \right) + \left(A_x(x,t) - \frac{E_0}{\kappa} \right) \sum_{n=-\infty}^{\infty} |c_n|^2 \exp \left(-\kappa^2(x - n x_0)^2 \right), \\ \frac{\partial^2 A_y(x,t)}{\partial x^2} &= \eta \frac{\partial A_y(x,t)}{\partial t} + \sum_{n=-\infty}^{\infty} (A_y(x,t) - 2 \pi \kappa n) |c_n|^2 \exp \left(-\kappa^2(x - n x_0)^2 \right), \\ \frac{\partial^2 A_z(x,t)}{\partial x^2} &= \eta \frac{\partial A_z(x,t)}{\partial t} + \sum_{n=-\infty}^{\infty} |c_n|^2 \exp \left(-\kappa^2(x - n x_0)^2 \right). \end{aligned} \tag{150}$$

Let us now consider an expansion to linear order in E_0 . In order to obtain a more explicit solution for the order parameter (148), we have to estimate the summations

$$\begin{aligned} \sum_{n=-\infty}^{\infty} |c_n|^2 \exp \left(-\kappa^2(x - n x_0)^2 \right) \\ \sum_{n=-\infty}^{\infty} n |c_n|^2 \exp \left(-\kappa^2(x - n x_0)^2 \right). \end{aligned} \tag{151}$$

Since we are interested in high- T_c superconductors featuring a square vortex lattice, we replace the general coefficients c_n with the correspondent c_{\square} that, in the considered framework, reads [131]

$$c_{\square}^2 = 2 \sqrt{2\pi} \kappa^2. \tag{152}$$

being then a constant function of $\kappa = \lambda/\xi$.

For high- T_c superconductors, the κ parameter is usually large, $\kappa^2 \gtrsim 10^4$: this in turn implies for the above (151):

$$\begin{aligned} \sum_{n=-\infty}^{\infty} |c_n|^2 \exp \left(-\kappa^2(x - n x_0)^2 \right) &= c_{\square}^2 e^{-\kappa^2 x^2} \sum_{n=-\infty}^{\infty} e^{-\kappa^2 n^2 x_0^2} e^{2x x_0 n \kappa^2} \simeq c_{\square}^2 e^{-\kappa^2 x^2}, \\ \sum_{n=-\infty}^{\infty} n |c_n|^2 \exp \left(-\kappa^2(x - n x_0)^2 \right) &\simeq 0, \end{aligned} \tag{153}$$

where the summation on the first line receives a non-negligible contribution only from the $n = 0$ term.

The Equation (150) for the vector potential can be now recast as

$$\begin{aligned} \frac{\partial^2 A_x(x,t)}{\partial x^2} &= \eta \left(\frac{\partial A_x(x,t)}{\partial t} - E_0 \right) + \left(A_x(x,t) - \frac{E_0}{\kappa} \right) c_{\square}^2 e^{-\kappa^2 x^2}, \\ \frac{\partial^2 A_y(x,t)}{\partial x^2} &= \eta \frac{\partial A_y(x,t)}{\partial t} + A_y(x,t) c_{\square}^2 e^{-\kappa^2 x^2}, \\ \frac{\partial^2 A_z(x,t)}{\partial x^2} &= \eta \frac{\partial A_z(x,t)}{\partial t} + c_{\square}^2 e^{-\kappa^2 x^2}. \end{aligned} \tag{154}$$

Since we are considering high- T_c superconductors ($\kappa^2 \gtrsim 10^4$), it is also possible to approximate

$$e^{-\kappa^2 x^2} \simeq \frac{\sqrt{\pi}}{\kappa} \delta(x), \tag{155}$$

so that the above expressions read

$$\frac{\partial A_x(x, t)}{\partial t} \simeq \frac{1}{\eta} \frac{\partial^2 A_x(x, t)}{\partial x^2} - \left(A_x(x, t) - \frac{E_0}{\kappa} \right) c_{\square}^2 \frac{\sqrt{\pi}}{\eta \kappa} \delta(x) + E_0, \tag{156a}$$

$$\frac{\partial A_y(x, t)}{\partial t} \simeq \frac{1}{\eta} \frac{\partial^2 A_y(x, t)}{\partial x^2} - A_y(x, t) c_{\square}^2 \frac{\sqrt{\pi}}{\eta \kappa} \delta(x), \tag{156b}$$

$$\frac{\partial A_z(x, t)}{\partial t} \simeq \frac{1}{\eta} \frac{\partial^2 A_z(x, t)}{\partial x^2} - c_{\square}^2 \frac{\sqrt{\pi}}{\eta \kappa} \delta(x). \tag{156c}$$

The initial conditions for the vector potential components are:

$$A_x(x, 0) = 0 \quad A_y(x, 0) = B_0 x \quad A_z(x, 0) = 0 \tag{157}$$

and the generalized electric field \mathbf{E} inside the superfluid is given by

$$\mathbf{E} = -\frac{\partial \mathbf{A}}{\partial t} - \nabla \phi. \tag{158}$$

5.3.3. Averaged Solutions

We now consider the spatial averaged effects, determined by the presence of generalized field and potentials, inside the supercondensate region. This can be obtained integrating the vector potential components (156) over the x -variable [133].

First, we integrate Equation (156c) over x in the interval $x \in [-L/2, L/2]$, obtaining

$$\frac{\partial \bar{A}_z(t)}{\partial t} = -c_{\square}^2 \frac{\sqrt{\pi}}{\eta \kappa L}, \tag{159}$$

having introduced the averaged component

$$\bar{A}_z(t) = \frac{1}{L} \int_{-L/2}^{L/2} dx A_z(x, t), \tag{160}$$

and taking advantage of symmetric conditions for the first derivatives with respect to x . Let us also keep in mind that we are dealing with the *dimensionless* quantities, having dropped the primes for the sake of notational simplicity (In particular, the x coordinate corresponds to the dimensionless x' of (106), while one would explicitly have for the dimensionless thickness $L' = L/\lambda$, L being the physical thickness and λ the penetration depth). The above (160) is solved by

$$\bar{A}_z(t) = -c_{\square}^2 \frac{\sqrt{\pi}}{\eta \kappa L} t + \bar{A}_z(0) = -c_{\square}^2 \frac{\sqrt{\pi}}{\eta \kappa L} t, \tag{161}$$

where initial conditions (157) implies $\bar{A}_z(0) = 0$. The averaged, generalized electric field \bar{E}_z component is then given by

$$\bar{E}_z = c_{\square}^2 \frac{\sqrt{\pi}}{\eta \kappa L} = \frac{2\sqrt{2} \pi \kappa}{\eta L}. \tag{162}$$

having used (158) and (144).

The averaged differential equation for the $\bar{A}_y(t)$ component, defined in the same way as (160), is obtained from (156b) and reads

$$\frac{\partial \bar{A}_y(t)}{\partial t} = -\bar{A}_y(t) c_{\square}^2 \frac{\sqrt{\pi}}{\eta \kappa L}, \tag{163}$$

having used the approximation $A_y(0, t) \simeq \bar{A}_y(t)$. The resulting averaged component reads

$$\bar{A}_y(t) = \bar{A}_y(0) \exp\left(-c_{\square}^2 \frac{\sqrt{\pi}}{\eta \kappa L} t\right) = 0, \tag{164}$$

having again used initial condition (157). This also implies that the electric field $\bar{E}_y(t)$ component is vanishing,

$$\bar{E}_y(t) = 0. \tag{165}$$

The equation for the vertical component comes from the (156a) expression and reads

$$\frac{\partial \bar{A}_x(t)}{\partial t} = -\left(\frac{\bar{A}_x(t)}{L} - \frac{E_0}{\kappa}\right) c_{\square}^2 \frac{\sqrt{\pi}}{\eta \kappa} + E_0, \tag{166}$$

Using again the approximation $A_x(0, t) \simeq \bar{A}_x(t)$ and the initial conditions (157), we find for the $\bar{A}_x(t)$ solution

$$\begin{aligned} \bar{A}_x(t) &= \bar{A}_x(0) \exp\left(-c_{\square}^2 \frac{\sqrt{\pi}}{\eta \kappa L} t\right) + E_0 \left(\frac{L}{\kappa} + \frac{\eta \kappa L}{c_{\square}^2 \sqrt{\pi}}\right) \left(1 - \exp\left(-c_{\square}^2 \frac{\sqrt{\pi}}{\eta \kappa L} t\right)\right) = \\ &= E_0 \left(\frac{L}{\kappa} + \frac{\eta \kappa L}{c_{\square}^2 \sqrt{\pi}}\right) \left(1 - \exp\left(-c_{\square}^2 \frac{\sqrt{\pi}}{\eta \kappa L} t\right)\right) \end{aligned} \tag{167}$$

Finally, the averaged $E_x(t)$ component along the vertical direction for the generalized electric field comes from Formulas (158) and (144) and reads

$$\begin{aligned} \bar{E}_x(t) &= E_0 - E_0 \left(\frac{L}{\kappa} + \frac{\eta \kappa L}{c_{\square}^2 \sqrt{\pi}}\right) c_{\square}^2 \frac{\sqrt{\pi}}{\eta \kappa L} \exp\left(-c_{\square}^2 \frac{\sqrt{\pi}}{\eta \kappa L} t\right) = \\ &= E_0 - E_0 \left(\frac{2\sqrt{2}\pi}{\eta} + 1\right) \exp\left(-\frac{2\sqrt{2}\pi \kappa}{\eta L} t\right). \end{aligned} \tag{168}$$

5.3.4. Expected Effects

The analysis of the averaged effect inside the supercondensate region shows some interesting predictions.

The first effect is the emergence of a new component of the (generalized) electric field, parallel to the superconductor surface and directed along the external applied magnetic field. The value of this new contribution is found using the (dimensionless) result (162) together with Formula (107), and in dimensional units reads

$$E_z = \frac{4\pi B_C(T) \mathcal{D}}{\eta L}. \tag{169}$$

If we consider a $\text{Bi}_2\text{Sr}_2\text{Ca}_3\text{Cu}_3\text{O}_{10}$ sample ($T_c \simeq 107\text{ K}$, $\lambda_0 \simeq 2.4 \times 10^{-7}\text{ m}$, $\xi_0 \simeq 1\text{ nm}$,

$\sigma^{-1} \simeq 3.6 \times 10^{-6} \Omega \text{ m}$, $\mathcal{D} \simeq 10^{-3} \text{ m}^2/\text{s}$ [134,135]) of thickness $L = 15 \text{ cm}$ at a temperature $T = 102 \text{ K}$; this would correspond to a resulting field

$$T \simeq 102 \text{ K} : \quad E_z = \frac{4\pi B_c(T) \mathcal{D}}{\eta L} = \frac{4\pi B_c(T)}{\mu_0 \sigma L} \simeq 77 \frac{\text{V}}{\text{m}}, \quad (170)$$

with $B_c(T) \simeq 0.32 \text{ Tesla}$.

The second expected effect is affection of the local gravitational field along the x direction in the supercondensate region. The averaged effect is expressed by Equation (168), from which it is possible to appreciate the predicted, temporary alteration of the local field.

In Figure 9, we plot the field variation *inside* the superfluid region for two samples of different dimensions. Analogous with the results of Section 4 about the local alteration *outside* the material, we can see that, for very short time scales, the gravitational field has a non-negligible reduction. Clearly, sample dimensions and chemical composition play a key role in maximizing the effect.

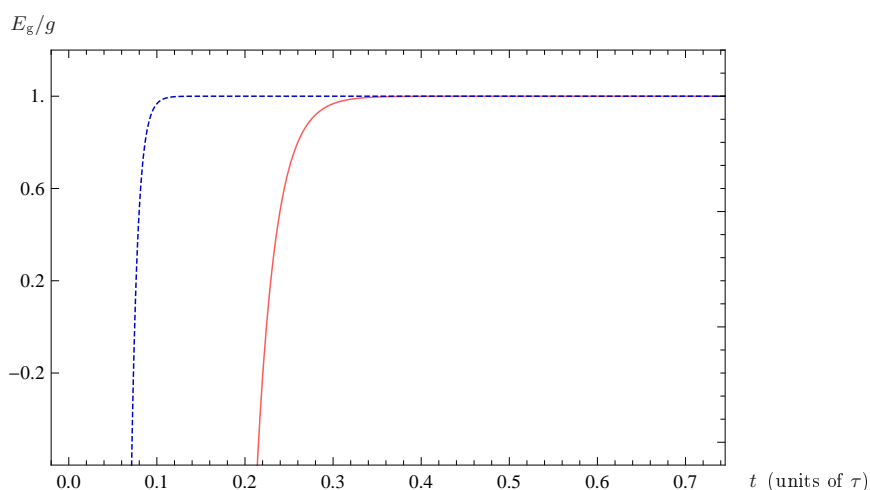


Figure 9. Local field variation as a function of time for a $\text{Bi}_2\text{Sr}_2\text{Ca}_3\text{Cu}_3\text{O}_{10}$ sample ($T_c \simeq 107 \text{ K}$, $\lambda_0 \simeq 2.4 \times 10^{-7} \text{ m}$, $\sigma^{-1} \simeq 3.6 \times 10^{-6} \Omega \text{ m}$, $\mathcal{D} \simeq 10^{-3} \text{ m}^2/\text{s}$, $\xi_0 \simeq 1 \text{ nm}$ [134,135]) at a temperature $T = 102 \text{ K}$. The red solid line refers to a sample of thickness $L = 15 \text{ cm}$, while the blue dashed line shows the result for $L = 5 \text{ cm}$.

First, we can appreciate that larger samples (i.e., larger values of L) would determine an increase of the time scales in which the effect manifests itself. In the same way, (168) suggests that large values of the η parameter, sample characteristics, determine an analogous increase of time ranges. The analysis then shows that L and η parameters determine similar effects: choosing a sample of reduced dimension (small L) of disordered material (small η , bad conductors in the normal state) would result in very short time scales, with a slight enhancement of the effect. Again, appropriate physical cutoffs should come into play, preventing non-physical growth of instabilities within the supercondensate, which would in turn lead to local field alterations of arbitrary intensity.

Since experimental issues would reside in the very short observation times, it is useful to take advantage of effects determined by the internal disorder. The effects of the latter can be easily understand, since material disorder causes an increase of the λ penetration depth. This, in turn, dictates an extension of the typical time scale τ of duration being $\tau \propto \lambda^2$, see definitions (105) and (138).

Finally, if the system is put at temperatures very close to T_c ; this is again an increase of the λ parameter and related larger time scales. In the latter case, however, the effects of thermal fluctuations should also be taken into account [136]. The described effects occur

analogous with what we found in Section 4 for the affection of the local field just outside the sample.

6. Conclusions

A deeper intertwining of different scientific areas has always proved to be a powerful tool for improving our understanding of many fascinating physical aspects of our world, see e.g., [137–159]. The intriguing existence of an interplay between gravity and superconductivity has been investigated by many researchers in the last decades, due to the enormous conceptual implications and many possible applications. In particular, the interaction has been theoretically predicted by numerous authors, with very different approaches and techniques. The phenomenon was then successfully tested in relation to the effects of gravitational perturbation on supercurrents and supercondensates, having used the latter as “gravitational antennas” for the detection of gravitational waves.

In this review, we mainly focused on the possible back-reaction exerted by the superfluid on the surrounding gravitational field, trying to provide qualitative and quantitative predictions about the extent of the proposed effect. Inspired by theoretical and experimental studies on gravity-induced generalized fields in superconductors, we studied the possible alterations exploiting a gravito–Maxwell formalism, integrated with the Ginzburg–Landau theory of phase transitions for superconducting systems. The latter formalism is a phenomenological theory, the superconducting materials being characterized by parameters which, in principle, can be optimized to enhance specific effects.

Clearly, there is still a lot of work to be done in order to better define the ranges and magnitude of the effect, as well as to determine optimal situations from an experimental point of view. In this regard, a crucial role would be played by suitable samples geometry, external electromagnetic fields of adequate frequency and appropriate characteristics of the material. In the future, 2D materials with variable number of layers should also be taken into consideration, in order to exploit their peculiar properties [160,161].

Author Contributions: Both authors contributed equally to conceptualization, methodology, formal analysis, original draft preparation and writing. All authors have read and agreed to the published version of the manuscript.

Funding: This research received no external funding.

Acknowledgments: G.A. Ummarino acknowledges partial support from the MEPhI. We also thank Fondazione CRT that partially supported this work for A. Gallerati.

Conflicts of Interest: The authors declare no conflict of interest.

References

1. DeWitt, B.S. Superconductors and gravitational drag. *Phys. Rev. Lett.* **1966**, *16*, 1092–1093. [[CrossRef](#)]
2. Papini, G. London moment of rotating superconductors and Lense-Thirring fields of general relativity. *Il Nuovo Cimento B* **1966**, *45*, 66–68. [[CrossRef](#)]
3. Papini, G. Detection of inertial effects with superconducting interferometers. *Phys. Lett. A* **1967**, *24*, 32–33. [[CrossRef](#)]
4. Hirakawa, H. Superconductors in gravitational field. *Phys. Lett. A* **1975**, *53*, 395–396. [[CrossRef](#)]
5. Ciubotariu, C. Absorption of gravitational waves. *Phys. Lett. A* **1991**, *158*, 27–30. [[CrossRef](#)]
6. Anandan, J. Relativistic gravitation and superconductors. *Class. Quant. Grav.* **1994**, *11*, 23. [[CrossRef](#)]
7. Podkletnov, E.; Nieminen, R. A possibility of gravitational force shielding by bulk $\text{YBa}_2\text{Cu}_3\text{O}_{7-x}$ superconductor. *Phys. C Supercond.* **1992**, *203*, 441–444. [[CrossRef](#)]
8. Modanese, G. Theoretical analysis of a reported weak gravitational shielding effect. *Europhys. Lett.* **1996**, *35*, 413–418. [[CrossRef](#)]
9. Modanese, G. Role of a ‘local’ cosmological constant in Euclidean quantum gravity. *Phys. Rev. D* **1996**, *54*, 5002–5009. [[CrossRef](#)] [[PubMed](#)]
10. Agop, M.; Buzea, C.; Griga, V.; Ciubotariu, C.; Stan, C.; Jatimir, D. Gravitational paramagnetism, diamagnetism and gravitational superconductivity. *Aust. J. Phys.* **1996**, *49*, 1063–1074. [[CrossRef](#)]

11. Li, N.; Torr, D. Effects of a gravitomagnetic field on pure superconductors. *Phys. Rev. D* **1991**, *43*, 457. [[CrossRef](#)] [[PubMed](#)]
12. Ahmedov, B. General relativistic thermoelectric effects in superconductors. *Gen. Relativ. Gravit.* **1999**, *31*, 357–369. [[CrossRef](#)]
13. Agop, M.; Ioannou, P.; Diaconu, F. Some implications of gravitational superconductivity. *Prog. Theor. Phys.* **2000**, *104*, 733–742. [[CrossRef](#)]
14. Modanese, G. Local contribution of a quantum condensate to the vacuum energy density. *Mod. Phys. Lett. A* **2003**, *18*, 683–690. [[CrossRef](#)]
15. Wu, N. Gravitational shielding effects in gauge theory of gravity. *Commun. Theor. Phys.* **2004**, *41*, 567–572. [[CrossRef](#)]
16. Hathaway, G.; Cleveland, B.; Bao, Y. Gravity modification experiment using a rotating superconducting disk and radio frequency fields. *Phys. C Supercond.* **2003**, *385*, 488. [[CrossRef](#)]
17. Kiefer, C.; Weber, C. On the interaction of mesoscopic quantum systems with gravity. *Ann. Phys.* **2005**, *14*, 253–278. [[CrossRef](#)]
18. Quach, J.Q. Gravitational Casimir effect. *Phys. Rev. Lett.* **2015**, *114*, 081104, Erratum: *Phys. Rev. Lett.* **2017**, *118*, 139901. [[CrossRef](#)]
19. Ummarino, G.A.; Gallerati, A. Superconductor in a weak static gravitational field. *Eur. Phys. J. C* **2017**, *77*, 549. [[CrossRef](#)]
20. Atanasov, V. The geometric field (gravity) as an electro-chemical potential in a Ginzburg-Landau theory of superconductivity. *Phys. B Condens. Matter* **2017**, *517*, 53–58. [[CrossRef](#)]
21. Atanasov, V. Gravitation at the Josephson junction. *Adv. Cond. Matt. Phys.* **2018**, *2018*, 1618252. [[CrossRef](#)]
22. Papini, G. Superconducting and normal metals as detectors of gravitational waves. *Lett. Nuovo Cim.* **1970**, *4S1*, 1027–1032. [[CrossRef](#)]
23. Adler, R.J. Long conductors as antennae for gravitational radiation. *Nature* **1976**, *259*, 296–297. [[CrossRef](#)]
24. Anandan, J. Relativistic thermoelectromagnetic gravitational effects in normal conductors and superconductors. *Phys. Lett. A* **1984**, *105*, 280–284. [[CrossRef](#)]
25. Anandan, J. Detection of gravitational radiation using superconducting circuits. *Phys. Lett. A* **1985**, *110*, 446–450. [[CrossRef](#)]
26. Carelli, P.; Castellano, M.; Cosmelli, C.; Foglietti, V.; Modena, I. Coupling of a high-sensitivity superconducting amplifier to a gravitational-wave antenna. *Phys. Rev. A* **1985**, *32*, 3258. [[CrossRef](#)] [[PubMed](#)]
27. Chan, H.; Paik, H. Superconducting gravity gradiometer for sensitive gravity measurements. I. Theory. *Phys. Rev. D* **1987**, *35*, 3551. [[CrossRef](#)] [[PubMed](#)]
28. Mashhoon, B.; Paik, H.J.; Will, C.M. Detection of the gravitomagnetic field using an orbiting superconducting gravity gradiometer. Theoretical principles. *Phys. Rev. D* **1989**, *39*, 2825. [[CrossRef](#)] [[PubMed](#)]
29. Preparata, G. ‘Superradiance’ Effects in a Gravitational Antenna. *Mod. Phys. Lett. A* **1990**, *5*, 1. [[CrossRef](#)]
30. Peng, H. The effects of gravitational waves on a superconducting antenna and its sensitivity. *Gen. Rel. Grav.* **1990**, *22*, 33–43. [[CrossRef](#)]
31. Peng, H.; Torr, D. The Electric field induced by a gravitational wave in a superconductor: A Principle for a new gravitational wave antenna. *Gen. Rel. Grav.* **1990**, *22*, 53–59. [[CrossRef](#)]
32. Peng, H.; Chin, Y.; Lind, G. Interaction between gravity and moving superconductors. *Gen. Rel. Grav.* **1991**, *23*, 1231–1250. [[CrossRef](#)]
33. Peng, H.; Torr, D.; Hu, E.; Peng, B. Electrodynamics of moving superconductors and superconductors under the influence of external forces. *Phys. Rev. B* **1991**, *43*, 2700. [[CrossRef](#)] [[PubMed](#)]
34. Li, F.; Baker, R., Jr. Detection of high-frequency gravitational waves by superconductors. *Int. J. Mod. Phys. B* **2007**, *21*, 3274–3278. [[CrossRef](#)]
35. Minter, S.J.; Wegter-McNelly, K.; Chiao, R.Y. Do Mirrors for Gravitational Waves Exist? *Phys. E* **2010**, *42*, 234. [[CrossRef](#)]
36. Inan, N.; Thompson, J.; Chiao, R. Interaction of gravitational waves with superconductors. *Fortschr. Phys.* **2017**, *65*, 1600066. [[CrossRef](#)]
37. Inan, N. A new approach to detecting gravitational waves via the coupling of gravity to the zero-point energy of the phonon modes of a superconductor. *Int. J. Mod. Phys. D* **2017**, *26*, 1743031. [[CrossRef](#)]
38. Hammad, F.; Landry, A. A simple superconductor quantum interference device for testing gravity. *Mod. Phys. Lett. A* **2020**, *35*, 2050171. [[CrossRef](#)]
39. Overhauser, A.; Colella, R. Experimental test of gravitationally induced quantum interference. *Phys. Rev. Lett.* **1974**, *33*, 1237. [[CrossRef](#)]
40. Colella, R.; Overhauser, A.; Werner, S. Observation of gravitationally induced quantum interference. *Phys. Rev. Lett.* **1975**, *34*, 1472–1474. [[CrossRef](#)]
41. Anandan, J. Gravitational and Rotational Effects in Quantum Interference. *Phys. Rev. D* **1977**, *15*, 1448–1457. [[CrossRef](#)]
42. Anandan, J. Interference, Gravity and Gauge Fields. *Nuovo Cim. A* **1979**, *53*, 221. [[CrossRef](#)]
43. Anandan, J. Gravitationally Coupled Electromagnetic Systems and Quantum Interference. *Class. Quant. Grav.* **1984**, *1*, L51. [[CrossRef](#)]
44. Cai, Y.; Papini, G. Particle Interferometry in Weak Gravitational Fields. *Class. Quant. Grav.* **1989**, *6*, 407. [[CrossRef](#)]

45. Ahluwalia, D.; Burgard, C. Gravitationally induced quantum mechanical phases and neutrino oscillations in astrophysical environments. *Gen. Rel. Grav.* **1996**, *28*, 1161–1170. [[CrossRef](#)]
46. Bhattacharya, T.; Habib, S.; Mottola, E. Gravitationally induced neutrino oscillation phases in static space-times. *Phys. Rev. D* **1999**, *59*, 067301. [[CrossRef](#)]
47. Müntinga, H.; Ahlers, H.; Krutzik, M.; Wenzlawski, A.; Arnold, S.; Becker, D.; Bongs, K.; Dittus, H.; Duncker, H.; Gaaloul, N.; et al. Interferometry with Bose-Einstein Condensates in Microgravity. *Phys. Rev. Lett.* **2013**, *110*, 093602. [[CrossRef](#)] [[PubMed](#)]
48. Asenbaum, P.; Overstreet, C.; Kovachy, T.; Brown, D.D.; Hogan, J.M.; Kasevich, M.A. Phase Shift in an Atom Interferometer due to Spacetime Curvature across its Wave Function. *Phys. Rev. Lett.* **2017**, *118*, 183602. [[CrossRef](#)]
49. Kiefer, C.; Singh, T.P. Quantum gravitational corrections to the functional Schrodinger equation. *Phys. Rev. D* **1991**, *44*, 1067–1076. [[CrossRef](#)] [[PubMed](#)]
50. Sakurai, J.J.; Napolitano, J. *Modern Quantum Mechanics*; Cambridge University Press: Cambridge, UK, 2017.
51. Schiff, L.; Barnhill, M. Gravitation-induced electric field near a metal. *Phys. Rev.* **1966**, *151*, 1067. [[CrossRef](#)]
52. Witteborn, F.; Fairbank, W. Experimental comparison of the gravitational force on freely falling electrons and metallic electrons. *Phys. Rev. Lett.* **1967**, *19*, 1049. [[CrossRef](#)]
53. Witteborn, F.; Fairbank, W. Experiments to determine the force of gravity on single electrons and positrons. *Nature* **1968**, *220*, 436–440. [[CrossRef](#)]
54. Beams, J. Potentials on rotor surfaces. *Phys. Rev. Lett.* **1968**, *21*, 1093. [[CrossRef](#)]
55. Herring, C. Gravitationally induced electric field near a conductor, and its relation to the surface-stress concept. *Phys. Rev.* **1968**, *171*, 1361. [[CrossRef](#)]
56. Peshkin, M. Gravity-induced electric field near a conductor. *Ann. Phys.* **1968**, *46*, 1–11. [[CrossRef](#)]
57. Peshkin, M. Gravity-induced electric field near a conductor. *Phys. Lett. A* **1969**, *29*, 181–182. [[CrossRef](#)]
58. Craig, P.P. Direct observation of stress-induced shifts in contact potentials. *Phys. Rev. Lett.* **1969**, *22*, 700. [[CrossRef](#)]
59. Rieger, T. Gravitationally Induced Electric Field in Metals. *Phys. Rev. B* **1970**, *2*, 825. [[CrossRef](#)]
60. Leung, M. Electric fields induced by gravitational fields in metals. *Il Nuovo Cimento B* **1972**, *7*, 220–224. [[CrossRef](#)]
61. Lockhart, J.; Witteborn, F.; Fairbank, W. Evidence for a temperature-dependent surface shielding effect in Cu. *Phys. Rev. Lett.* **1977**, *38*, 1220. [[CrossRef](#)]
62. Anandan, J. New relativistic gravitational effects using charged-particle interferometry. *Gen. Rel. Grav.* **1984**, *16*, 33–41. [[CrossRef](#)]
63. Peng, H. On calculation of magnetic-type gravitation and experiments. *Gen. Relativ. Gravit.* **1983**, *15*, 725–735. [[CrossRef](#)]
64. Jain, A.; Lukens, J.; Tsai, J. Test for relativistic gravitational effects on charged particles. *Phys. Rev. Lett.* **1987**, *58*, 1165–1168. [[CrossRef](#)] [[PubMed](#)]
65. Li, N.; Torr, D. Gravitational effects on the magnetic attenuation of superconductors. *Phys. Rev. B* **1992**, *46*, 5489. [[CrossRef](#)] [[PubMed](#)]
66. Harris, E. Analogy between general relativity and electromagnetism for slowly moving particles in weak gravitational fields. *Am. J. Phys.* **1991**, *59*, 421–425. [[CrossRef](#)]
67. Torr, D.; Li, N. Gravitoelectric-electric coupling via superconductivity. *Found. Phys. Lett.* **1993**, *6*, 371–383. [[CrossRef](#)]
68. Agop, M.; Buzea, C.; Nica, P. Local gravitoelectromagnetic effects on a superconductor. *Phys. C Supercond.* **2000**, *339*, 120–128. [[CrossRef](#)]
69. Tajmar, M.; De Matos, C. Gravitomagnetic field of a rotating superconductor and of a rotating superfluid. *Phys. C* **2003**, *385*, 551–554. [[CrossRef](#)]
70. Tajmar, M.; de Matos, C. Extended analysis of gravitomagnetic fields in rotating superconductors and superfluids. *Phys. C* **2005**, *420*, 56. [[CrossRef](#)]
71. Ahmedov, B.; Kagramanova, V. Electromagnetic effects in superconductors in stationary gravitational field. *Int. J. Mod. Phys. D* **2005**, *14*, 837–847. [[CrossRef](#)]
72. De Matos, C.J. Gravitational force between two electrons in superconductors. *Phys. C Supercond.* **2008**, *468*, 229–232. [[CrossRef](#)]
73. Tajmar, M. Electrodynamics in superconductors explained by Proca equations. *Phys. Lett. A* **2008**, *372*, 3289–3291. [[CrossRef](#)]
74. Misner, C.W.; Thorne, K.; Wheeler, J. *Gravitation*; W. H. Freeman: San Francisco, CA, USA, 1973.
75. Wald, R.M. *General Relativity*; Chicago University Press: Chicago, IL, USA, 1984. [[CrossRef](#)]
76. Ummarino, G.A.; Gallerati, A. Exploiting weak field gravity-Maxwell symmetry in superconductive fluctuations regime. *Symmetry* **2019**, *11*, 1341. [[CrossRef](#)]
77. Ummarino, G.A.; Gallerati, A. Josephson AC effect induced by weak gravitational field. *Class. Quant. Grav.* **2020**, *37*, 217001. [[CrossRef](#)]
78. Braginsky, V.B.; Caves, C.M.; Thorne, K.S. Laboratory Experiments to Test Relativistic Gravity. *Phys. Rev. D* **1977**, *15*, 2047. [[CrossRef](#)]
79. Ross, D. The London equations for superconductors in a gravitational field. *J. Phys. A* **1983**, *16*, 1331. [[CrossRef](#)]

80. Thorne, K. Gravitomagnetism, jets in quasars, and the stanford gyroscope experiment. In *Near Zero: New Frontiers of Physics*; W.H. Freeman & Co.: New York, NY, USA, 1988; pp. 573–586.
81. Peng, H. A new approach to studying local gravitomagnetic effects on a superconductor. *Gen. Relativ. Gravit.* **1990**, *22*, 609–617. [[CrossRef](#)]
82. Ruggiero, M.L.; Tartaglia, A. Gravitomagnetic effects. *Nuovo Cim. B* **2002**, *117*, 743–768.
83. Tartaglia, A.; Ruggiero, M.L. Gravitoelectromagnetism versus electromagnetism. *Eur. J. Phys.* **2004**, *25*, 203–210. [[CrossRef](#)]
84. Vieira, R.; Brentan, H. Covariant theory of gravitation in the framework of special relativity. *Eur. Phys. J. Plus* **2018**, *133*, 165. [[CrossRef](#)]
85. Behera, H. Comments on gravitoelectromagnetism of Ummarino and Gallerati in “Superconductor in a weak static gravitational field” vs other versions. *Eur. Phys. J. C* **2017**, *77*, 822. [[CrossRef](#)]
86. Giardino, S. A novel covariant approach to gravito-electromagnetism. *Braz. J. Phys.* **2020**, *50*, 372–378. [[CrossRef](#)]
87. Sbitnev, V.I. Quaternion algebra on 4D superfluid quantum space-time. Gravitomagnetism. *Found. Phys.* **2019**, *49*, 107–143. [[CrossRef](#)]
88. Gallerati, A. Interaction between superconductors and weak gravitational field. *J. Phys. Conf. Ser.* **2020**, *1690*, 012141. [[CrossRef](#)]
89. Williams, L.L.; Inan, N. Maxwellian mirages in general relativity. *New J. Phys.* **2021**, *23*, 053019. [[CrossRef](#)]
90. Gallerati, A. Local affection of weak gravitational field from supercondensates. *Phys. Scripta* **2021**, *96*, 064001. [[CrossRef](#)]
91. Toth, G.Z. Energy-momentum tensor and duality symmetry of linearized gravity in a Maxwellian formalism. *arXiv* **2021**, arXiv:2108.02124.
92. De Gennes, P.G. *Superconductivity of Metals and Alloys*; Taylor & Francis Ltd.: London, UK, 2018. [[CrossRef](#)]
93. Tinkham, M. *Introduction to Superconductivity*; Dover Publications Inc.: New York, NY, USA, 2004.
94. Ketterson, J.; Song, S. *Superconductivity*; Cambridge University Press: Cambridge, UK, 1999. [[CrossRef](#)]
95. Josephson, B. Possible new effects in superconductive tunnelling. *Phys. Lett.* **1962**, *1*, 251–253. [[CrossRef](#)]
96. Anderson, P. The Josephson Effect and Quantum Coherence Measurements in Superconductors and Superfluids. In *Progress in Low Temperature Physics*; Elsevier: Amsterdam, NL, USA, 1967; Volume 5, pp. 1–43.
97. Barone, A.; Paternò, G. *Physics and Applications of the Josephson Effect*; John Wiley & Sons: New York, NY, USA, 1982. [[CrossRef](#)]
98. Feynman, R.; Leighton, R.; Sands, M. The Josephson junction. In *The Feynman Lectures on Physics*; Addison-Wesley Publ. Comp.: New York, NY, USA, 1965; Chapter 21, Volume III.
99. Fossheim, K.; Sudbø, A. *Superconductivity: Physics and Applications*; John Wiley & Sons Ltd: Hoboken, NJ, USA, 2004. [[CrossRef](#)]
100. Gor’kov, L. Microscopic derivation of the Ginzburg-Landau equations in the theory of superconductivity. *Sov. Phys. JETP* **1959**, *9*, 1364–1367.
101. Josephson, B. Supercurrents through barriers. *Adv. Phys.* **1965**, *14*, 419–451. [[CrossRef](#)]
102. Josephson, B. Coupled superconductors. *Rev. Mod. Phys.* **1964**, *36*, 216. [[CrossRef](#)]
103. Ambegaokar, V.; Baratoff, A. tunnelling Between Superconductors. *Phys. Rev. Lett.* **1963**, *10*, 486. [[CrossRef](#)]
104. Ambegaokar, V.; Baratoff, A. tunnelling Between Superconductors (Errata). *Phys. Rev. Lett.* **1963**, *11*, 104. [[CrossRef](#)]
105. Saxena, A.K. The Proximity and Josephson Effects. In *High-Temperature Superconductors*; Springer: Berlin/Heidelberg, Germany, 2009; pp. 147–198. [[CrossRef](#)]
106. Bardeen, J.; Cooper, L.; Schrieffer, J. Theory of superconductivity. *Phys. Rev.* **1957**, *108*, 1175–1204. [[CrossRef](#)]
107. Ginzburg, V.; Landau, L. On the Theory of superconductivity. *Zh. Eksp. Teor. Fiz.* **1950**, *20*, 1064–1082.
108. Ginzburg, V.; Landau, L. On the Theory of Superconductivity. In *On Superconductivity and Superfluidity*; Springer: Berlin/Heidelberg, Germany, 2009; pp. 113–137. [[CrossRef](#)]
109. Ginzburg, V. Some remarks on phase transitions of the second kind and the microscopic theory of ferroelectric materials. *Soviet Phys. Solid State* **1961**, *2*, 1824–1834.
110. Thouless, D.J. Perturbation theory in statistical mechanics and the theory of superconductivity. *Ann. Phys.* **1960**, *10*, 553–588. [[CrossRef](#)]
111. Shier, J.; Ginsberg, D. Superconducting transitions of amorphous Bismuth alloys. *Phys. Rev.* **1966**, *147*, 384. [[CrossRef](#)]
112. Glover, R. Ideal resistive transition of a superconductor. *Phys. Lett. A* **1967**, *25*, 542–544. [[CrossRef](#)]
113. Strongin, M.; Kammerer, O.; Crow, J.; Thompson, R.; Fine, H. ‘Curie-Weiss’ behavior and fluctuation phenomena in the resistive transitions of dirty superconductors. *Phys. Rev. Lett.* **1968**, *20*, 922. [[CrossRef](#)]
114. Ferrell, R.; Schmidt, H. Predicted critical behavior near the superconducting phase transition. *Phys. Lett. A* **1967**, *25*, 544–545. [[CrossRef](#)]
115. Schmid, A. A time dependent Ginzburg-Landau equation and its application to the problem of resistivity in the mixed state. *Phys. Der Kondens. Mater.* **1966**, *5*, 302–317. [[CrossRef](#)]
116. Hurault, J. Nonlinear Effects on the Conductivity of a Superconductor above Its Transition Temperature. *Phys. Rev.* **1969**, *179*, 494. [[CrossRef](#)]
117. Schmid, A. Diamagnetic susceptibility at the transition to the superconducting state. *Phys. Rev.* **1969**, *180*, 527. [[CrossRef](#)]

118. Poole, C.K.; Farach, H.A.; Creswick, R.J. *Handbook of Superconductivity*; Academic Press: San Diego, CA, USA, 1999.
119. Welp, U.; Xie, R.; Koshelev, A.; Kwok, W.; Luo, H.; Wang, Z.; Mu, G.; Wen, H.H. Anisotropic phase diagram and strong coupling effects in $\text{Ba}_{1-x}\text{K}_x\text{Fe}_2\text{As}_2$ from specific-heat measurements. *Phys. Rev. B* **2009**, *79*, 094505. [[CrossRef](#)]
120. Ullah, S.; Dorsey, A. Effect of fluctuations on the transport properties of type-II superconductors in a magnetic field. *Phys. Rev. B* **1991**, *44*, 262. [[CrossRef](#)] [[PubMed](#)]
121. Tang, Q.; Wang, S. Time dependent Ginzburg-Landau equations of superconductivity. *Phys. D Nonlinear Phenom.* **1995**, *88*, 139–166. [[CrossRef](#)]
122. Du, Q.; Gray, P. High-kappa limits of the time-dependent Ginzburg-Landau model. *SIAM J. Appl. Math.* **1996**, *56*, 1060–1093. [[CrossRef](#)]
123. Lin, F.H.; Du, Q. Ginzburg-Landau vortices: dynamics, pinning, and hysteresis. *SIAM J. Math. Anal.* **1997**, *28*, 1265–1293. [[CrossRef](#)]
124. Fleckinger-Pellé, J.; Kaper, H.G.; Takáč, P. Dynamics of the Ginzburg-Landau equations of superconductivity. *Nonlinear Anal. Theory Methods Appl.* **1998**, *32*, 647–665. [[CrossRef](#)]
125. Kopnin, N.; Thuneberg, E. Time-dependent Ginzburg-Landau analysis of inhomogeneous normal-superfluid transitions. *Phys. Rev. Lett.* **1999**, *83*, 116. [[CrossRef](#)]
126. Ghinovker, M.; Shapiro, I.; Shapiro, B.Y. Explosive nucleation of superconductivity in a magnetic field. *Phys. Rev. B* **1999**, *59*, 9514. [[CrossRef](#)]
127. Ljubičić, A.; Logan, B. A proposed test of the general validity of Mach's principle. *Phys. Lett. A* **1992**, *172*, 3–5. [[CrossRef](#)]
128. Ummaryno, G.A.; Gallerati, A. Possible alterations of local gravitational field inside a superconductor. *Entropy* **2021**, *23*, 193. [[CrossRef](#)] [[PubMed](#)]
129. Kopnin, N.; Ivlev, B.; Kalatsky, V. The flux-flow Hall effect in type II superconductors. An explanation of the sign reversal. *J. Low Temp. Phys.* **1993**, *90*, 1–13. [[CrossRef](#)]
130. Kopnin, N. *Theory of Nonequilibrium Superconductivity*; Oxford University Press: Oxford, UK, 2001. [[CrossRef](#)]
131. Hoffmann, K.; Tang, Q. *Ginzburg-Landau Phase Transition Theory and Superconductivity*; Springer: Basel, Switzerland, 2012. [[CrossRef](#)]
132. Ummaryno, G.A.; Gallerati, A. Superconductor in static gravitational, electric and magnetic fields with vortex lattice. *Results Phys.* **2021**, *30*, 104838. [[CrossRef](#)]
133. Sanders, J.A.; Verhulst, F.; Murdock, J. *Averaging Methods in Nonlinear Dynamical Systems*; Springer: New York, NY, USA, 2007. [[CrossRef](#)]
134. Weigand, M.; Eisterer, M.; Giannini, E.; Weber, H. Mixed state properties of $\text{Bi}_2\text{Sr}_2\text{Ca}_2\text{Cu}_3\text{O}_{10+\delta}$ single crystals before and after neutron irradiation. *Phys. Rev. B* **2010**, *81*, 014516. [[CrossRef](#)]
135. Piriou, A.; Fasano, Y.; Giannini, E.; Fischer, Ø. Effect of oxygen-doping on $\text{Bi}_2\text{Sr}_2\text{Ca}_2\text{Cu}_3\text{O}_{10+\delta}$ vortex matter: crossover from electromagnetic to Josephson interlayer coupling. *Phys. Rev. B* **2008**, *77*, 184508. [[CrossRef](#)]
136. Larkin, A.; Varlamov, A. *Theory of fluctuations in superconductors*; Oxford University Press: Oxford, UK, 2005. [[CrossRef](#)]
137. Zurek, W. Cosmological experiments in condensed matter systems. *Phys. Rept.* **1996**, *276*, 177–221. [[CrossRef](#)]
138. Volovik, G. Superfluid $^3\text{He-B}$ and gravity. *Phys. B Condens. Matter* **1990**, *162*, 222–230. [[CrossRef](#)]
139. Volovik, G. Superfluid analogies of cosmological phenomena. *Phys. Rept.* **2001**, *351*, 195–348. [[CrossRef](#)]
140. Baeuerle, C.; Bunkov, Y.M.; Fisher, S.N.; Godfrin, H.; Pickett, G.R. Laboratory simulation of cosmic string formation in the early Universe using superfluid He-3. *Nature* **1996**, *382*, 332–334. [[CrossRef](#)]
141. Ruutu, V.; Eltsov, V.; Gill, A.; Kibble, T.; Krusius, M.; Makhlin, Y.; Placais, B.; Volovik, G.; Xu, W. Big bang simulation in superfluid He-3-b: Vortex nucleation in neutron irradiated superflow. *Nature* **1996**, *382*, 334. [[CrossRef](#)]
142. Garay, L.J.; Anglin, J.R.; Cirac, J.I.; Zoller, P. Black holes in Bose-Einstein condensates. *Phys. Rev. Lett.* **2000**, *85*, 4643–4647. [[CrossRef](#)] [[PubMed](#)]
143. Jacobson, T.A.; Volovik, G.E. Event horizons and ergoregions in He-3. *Phys. Rev. D* **1998**, *58*, 064021. [[CrossRef](#)]
144. Barcelo, C.; Liberati, S.; Visser, M. Analog gravity from Bose-Einstein condensates. *Class. Quant. Grav.* **2001**, *18*, 1137. [[CrossRef](#)]
145. Novello, M.; Visser, M.; Volovik, G.E. *Artificial Black Holes*; World Scientific: Singapore, 2002. [[CrossRef](#)]
146. Barcelo, C.; Liberati, S.; Visser, M. Analogue gravity. *Living Rev. Rel.* **2005**, *8*, 12. [[CrossRef](#)] [[PubMed](#)]
147. Carusotto, I.; Fagnocchi, S.; Recati, A.; Balbinot, R.; Fabbri, A. Numerical observation of Hawking radiation from acoustic black holes in atomic Bose-Einstein condensates. *New J. Phys.* **2008**, *10*, 103001. [[CrossRef](#)]
148. Mannarelli, M.; Manuel, C. Transport theory for cold relativistic superfluids from an analogue model of gravity. *Phys. Rev. D* **2008**, *77*, 103014. [[CrossRef](#)]
149. Boada, O.; Celi, A.; Latorre, J.I.; Lewenstein, M. Dirac Equation For Cold Atoms In Artificial Curved Spacetimes. *New J. Phys.* **2011**, *13*, 035002. [[CrossRef](#)]
150. Gallerati, A. Graphene properties from curved space Dirac equation. *Eur. Phys. J. Plus* **2019**, *134*, 202. [[CrossRef](#)]

151. Capozziello, S.; Pincak, R.; Saridakis, E.N. Constructing superconductors by graphene Chern-Simons wormholes. *Annals Phys.* **2018**, *390*, 303–333. [[CrossRef](#)]
152. Andrianopoli, L.; Cerchiai, B.L.; D’Auria, R.; Gallerati, A.; Noris, R.; Trigiante, M.; Zanelli, J. \mathcal{N} -extended $D = 4$ supergravity, unconventional SUSY and graphene. *JHEP* **2020**, *1*, 84. [[CrossRef](#)]
153. Gallerati, A. Supersymmetric theories and graphene. *PoS* **2021**, *390*, 662. [[CrossRef](#)]
154. Zaanen, J.; Liu, Y.; Sun, Y.W.; Schalm, K. *Holographic Duality in Condensed Matter Physics*; Cambridge University Press: Cambridge, UK, 2015. [[CrossRef](#)]
155. Franz, M.; Rozali, M. Mimicking black hole event horizons in atomic and solid-state systems. *Nat. Rev. Mater.* **2018**, *3*, 491–501. [[CrossRef](#)]
156. Kolobov, V.I.; Golubkov, K.; Muñoz de Nova, J.R.; Steinhauer, J. Observation of stationary spontaneous Hawking radiation and the time evolution of an analogue black hole. *Nat. Phys.* **2021**, *17*, 362–367. [[CrossRef](#)]
157. Sbitnev, V.I. Quaternion Algebra on 4D Superfluid Quantum Space-Time. Dirac’s Ghost Fermion Fields. *Found. Phys.* **2022**, *52*, 19. [[CrossRef](#)]
158. Gallerati, A. Negative-curvature spacetime solutions for graphene. *J. Phys. Condens. Matter* **2021**, *33*, 135501. [[CrossRef](#)] [[PubMed](#)]
159. Lambiase, G.; Papini, G. *The Interaction of Spin with Gravity in Particle Physics*; Springer Nature: Cham, Switzerland, 2021. [[CrossRef](#)]
160. Clark, J.; Khodel, V.; Zverev, M.; Yakovenko, V. Unconventional superconductivity in two-dimensional electron systems with long-range correlations. *Phys. Rep.* **2004**, *391*, 123–156. [[CrossRef](#)]
161. Uchihashi, T. Two-dimensional superconductors with atomic-scale thickness. *Supercond. Sci. Technol.* **2016**, *30*, 013002. [[CrossRef](#)]